LONGMOR LONGSHORE MODELLING AND APPLICATION

1. Introduction

This document describes various applications of the LONGMOR-model, which can be used to compute the coastline changes as function of time.

The LONGMOR-model is a numerical model (FORTRAN-code) which can compute the following parameters: water depth at the breaker line; wave height and wave incidence angle at the breaker line, sand transport in the breaker zone and corresponding coastline changes over time due to alongshore gradients of the sand transport rate in the breaker zone.

Typical problems that can be solved using the LONGMOR-model are:

1. accretion updrift of structure;
2. erosion down drift of structure;
3. accretion and erosion of mega-nourishment along beaches;
4. erosion of coastal extensions.

How to run LONGMOR-model

The LONGMOR-model can be run quite simply:

1. click on the Longmor2013-intel.exe file; this opens the prompt-command line
2. type the name of the input file: name.inp, enter
3. the model runs and produce an output file: name.out; this file can be imported in EXCEL for plotting
4. if the model does run, see diagnose-file; this gives information where an input mistake is made (usually the table length does match the number data specified; if 8 wave data rows are specified then the table number is nt=8).
5. comments can be given to the right of *; enter new line, type *; old input data can be stored in input file by placing * before each data row; old input data is then always available.

2. Description of LONGMOR-model

2.1 Basic equations

The LONGMOR1D-model (**Van Rijn, 1998, 2002, 2005**) is a coastline model based on the sediment balance equation for the littoral zone (roughly the surf zone) with alongshore length Δx, cross-shore length Δy_s and vertical layer thickness (h). The model computes coastline changes if the longshore transport rates are known.
Basically, the accretional and erosional processes along the coastline are the result of differences in onshore/offshore transport and gradients of longshore sand transport, induced by:

- changes of shoreline orientation (gradual or abrupt due to presence of bays and head-lands);
- changes of shoreface topography (local steep slopes, hollows, scarps, canyons);
- changes of wave-current conditions and mean sea level conditions;
- changes of sediment supply (sources like cliff erosion).

Coastline changes can be simply understood by considering the sediment continuity equation for the littoral zone (roughly the surf zone) with alongshore length Δx, cross-shore length Δy and vertical layer thickness (h), see **Figure 2.1.1**.
The sand volume balance reads:

$$h\,(\Delta y_s/\Delta t) + \Delta Q_{LS}/\Delta x - q_s = 0 \qquad (2.1)$$

with:
y = cross-shore coordinate, x= longshore coordinate,
y_s = shoreline position,
h = thickness of active littoral zone layer,
Q_{LS} = longshore transport rate or littoral drift (bed-load plus suspended load transport in volume including pores per unit time, in m^3/s) and,
q_s = source, sink or cross-shore transport contribution (in m^2/s).

Basically, Equation (2.1) states that a coastal section erodes if more sand is carried away than supplied; vice versa coastal accretion occurs if there is a net supply. Coastline changes are linearly related to the assumed depth (h) of the active zone.

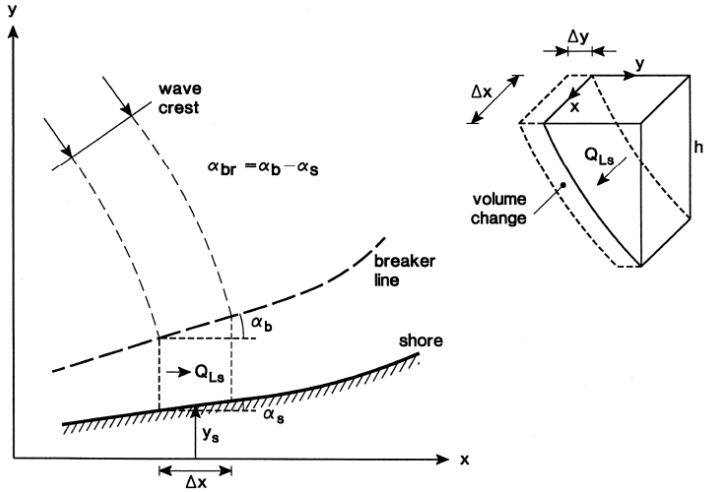

Figure 2.1.1 *Definition sketch of shoreline configuration and sand balance volume*

Three longshore sand transport equations are available.
The longshore sand transport of Van Rijn (2014) is described by:

$$Q_{LS}= 0.00018\ K\ K_{swell}\ (1-\varepsilon)^{-1}\ g^{0.5}\ (\tan\beta)^{0.4}\ (d_{50})^{-0.6}\ (H_{s,br})^{3.1}\ \sin(2\alpha_{br}) \qquad (2.2)$$

Q_{LS} = total longshore sediment transport (in m^3/s, incl. pores),
ε = porosity ($\cong$0.4), ρ_s =sediment density (kg/m^3),
d_{50} = median grain size (m),
$H_{s,br}$ = significant wave height at breaker line (m),
θ_{br} = wave angle at breaker line,
g = acceleration of gravity (m/s^2),
tanβ = slope of beach/surf zone,
K_{swell} = swell factor (see Equation 5),
K = calibration factor (default=1).

Equation (2.2) can also be expressed, as:

$$Q_{LS}= 0.0006\ K\ K_{swell}\ (1-\varepsilon)^{-1}\ (\tan\beta)^{0.4}\ (d_{50})^{-0.6}\ (H_{s,br})^{2.6}\ V_{eff,L} \qquad (2.3)$$

$$V_{wave}= 0.3\ \ (gH_{s,br})^{0.5}\ \sin(2\alpha_{br}) \qquad (2.4)$$

with:
$V_{eff,L}$ = $[(V_{wave,L})^2+(V_{tide,L})^2]^{0.5}$= effective longshore velocity at mid surf zone (m/s) for tidal velocity and wave induced velocity in same direction (minus sign for opposing conditions);
$V_{wave,L}$ = wave-induced longshore current velocity (m/s) averaged over the cross-section of the surf zone.
$V_{tide,L}$ = longshore velocity in mid surf zone due to tidal forcing (=0 m/s for non-tidal cases; 0.1 m/s for micro-tidal, 0.3 m/s for meso-tidal and 0.5 m/s for macro-tidal cases).

Equation (2.1) does not account for the effect of the wave period on the longshore transport rate. However, low-period swell waves in the range of 1 to 2 m produce significantly larger transport rates compared to wind waves of the same height (H_{rms}=H). This effect can to some extent be taken into account by using a correction factor to the longshore transport rate, if the percentage of swell waves (in terms of wave height) of the total wave height record is known.
Herein, it is proposed to use a swell factor, as follows:

$$K_{swell}=1.5(p_{swell}/100) + 1\ (1-p_{swell}/100) = 0.015p_{swell} + (1-0.01p_{swell}) \qquad (2.5)$$

with: p_{swell}= percentage of low-period swell wave heights of the total wave height record (about 10% to 20% for sea coasts and 20% to 30% for ocean coasts).
Some values are: K_{swell}=1.05 for p_{swell}=10%; K_{swell}=1.1 for p_{swell}=20% and K_{swell}=1.5 for p_{swell}=100%.
If swell is absent (or unknown), then K_{swell}= 1.
Using this approach, the longshore transport rate increases slightly with increasing percentage of swell. The swell factor is based on computations with grain sizes in the range of 0.2 to 50 mm.

The Kamphuis (1991) method is given by:

$$Q_{LS}=2.33\ K\ [\rho_s/(\rho_s-\rho)]\ [(1-\varepsilon)\rho_s]^{-1}\ (T_p)^{1.5}\ (\tan\beta)^{0.75}\ (d_{50})^{-0.25}\ (H_{s,br})^2\ [\sin(2\alpha_{br})]^{0.6} \quad (2.6)$$

with: Q_{LS}= longshore sediment (m^3/s, incl pores); $H_{s,br}$=significant wave height at breaker line (m); α_{br} =wave angle at breaker line (°); d_{50}=median particle size in surf zone (m); tan β= beach slope; T_p = peak wave period; K = calibration factor (default=1).

The longshore sand transport (Q_{LS}) of CERC (Shore Protection Manual 1984; Van Rijn, 1993):

$$Q_{LS}= 0.023\ K\ g^{0.5}\ \gamma^{-0.5}\ (H_{s,br})^{2.5}\ \sin(2\alpha_{br}) \quad (2.7)$$

with: γ= breaker coefficient, H_{br}= significant wave height at breaker line and α_{br}= angle between breaker line and local shoreline; K = calibration factor (default=1).

The longshore sand transport rate in the surf zone is defined in terms of parameters defined at the breaker line. Thus, the offshore wave climate has to be converted to a wave climate at the breaker line. **(The wave climate should be determined from measured or modeled data as close as possible to the shore!)**
Waves arriving from deeper water are transformed in shallow water according to the laws of energy flux conservation and refraction (Law of Snell) for gradually varying bathymetry, yielding (Van Rijn 2011);

$$\sin\alpha_{br}= (L_{br}/L_o)\ \sin\alpha_o \quad (2.8)$$
$$H_{br}= K_{r,br}\ K_{s,br}\ H_o \quad (2.9)$$

with $K_{r,br}$= refraction coefficient at breaker line and $K_{s,br}$= shoaling coefficient at breaker line.

For gradually varying bathymetry these values are:

$$K_{r,br}= (\cos\alpha_o/\cos\alpha_{br})^{0.5} \text{ and } K_{s,br}=(n_o c_o/n_{br} c_{br})^{0.5} \quad (2.10)$$

with c = wave propagation velocity, n = coefficient, α= wave angle, index br= at breaker line and index o= at deep water.
The wave height at the breaker line $H_{br} = \gamma h_{br}$ can be computed if the breaker depth h_{br} and the breaker coefficient γ (0.6-0.8 0.6) are known. Generally, this procedure requires iterative computations.
An estimate of the breaker depth can be obtained by applying (Van Rijn 2011):

$$h_{br}= ((H_o^2\ c_o\ \cos\alpha_o)/(1.8\gamma^2 g^{0.5}))^{0.4} \quad (2.11)$$

Thus, wave refraction largely controls the orientation of the shoreline, when relatively smooth and regular depth contours are present (neglecting cross-shore contributions).

The longshore transport rate along a specific coastal section depends on the angle α_o between the shoreline and the deep-water wave direction. If the shoreline orientation varies and the wave direction is constant, the longshore transport rate can be expressed as a function of α_o. This curve (including refraction and shoaling effects) is shown for a specific case in **Figure 2.1.2**. The transport rate is maximum for a shoreline orientation of about α_o = 40° to 45° (depending on refraction effects) and zero for angles of 0° (wave crests parallel to coast) and 90° (wave crests normal to coasts). The longshore transport will be in opposite direction (negative Q_{LS}) for

α_o <0°. The longshore transport can also be expressed as a function of the shoreline angle α_s ($\alpha_s = \alpha_n - \alpha_o$, α_n= constant if wave direction is constant and shoreline is varying, α_n=45° in the example of **Figure 2.2**) with respect to the x-axis. In the case of a wave climate with various wave classes, directions and probabilities of occurrence the net longshore transport rate can be expressed as a function of shoreline orientation.
Equation (1) is valid for wave-induced longshore transport in the absence of tide- or wind- driven currents. The effect of quasi-steady currents superimposed on the wave-induced longshore current will result in a vertical shift of the transport curve in **Figure 2.1.2**.

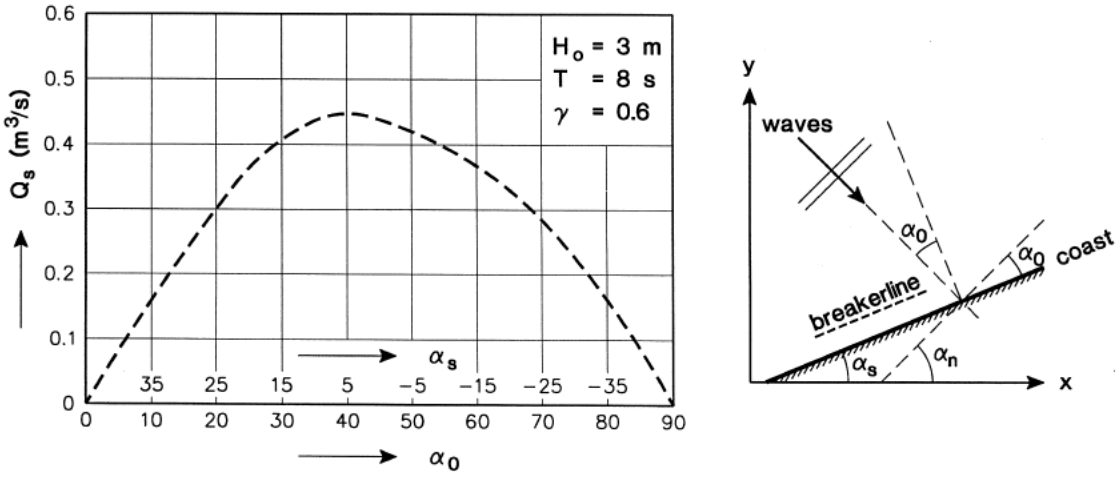

Figure 2.1.2 *Longshore transport rate as a function of shoreline orientation*
(α_o = angle between deep-water wave direction and shoreline)
(α_s= angle between shoreline and x-axis)

Definitions of directions in LONGNOR

- Longshore transport in positive x-direction is positive; this requires a positive wave angle to shore normal (**Figure 2.1.3**);
- Longshore transport in negative x-direction is negative positive; this requires a positive wave angle to shore normal.

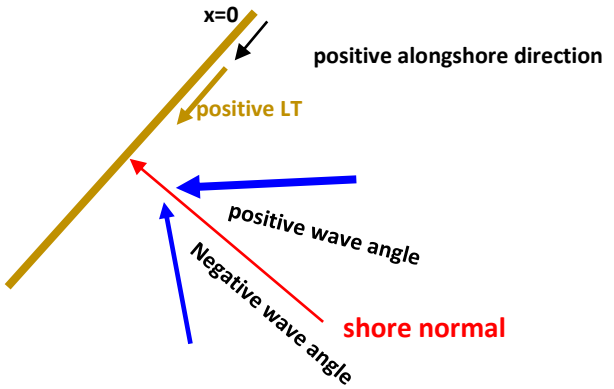

Figure 2.1.3 *Definitions of positive and negative longshore transport rate*

2.2 Numerical scheme

The mass balance equation (2.1) reads as:

$$h\,\Delta y_s/\Delta t + \Delta Q_{LS}/\Delta x - q_s = 0 \qquad (2.12)$$
$$\Delta y_s = [\Delta x\, q_s - \Delta Q_{LS}]\,[\Delta t/(h\,\Delta x)]$$

with:
Δy_s = coastline change (m),
Δt = time step (s), Δx = space step (m),
h = thickness active layer (5 to 10 m),
q_s = source/sink term (nourishment or sand mining) per unit coastline (in $m^3/(ms)$),
Q_{LS} = longshore sand transport including pores (in m^3/s).

Deposition if $\Delta Q_{LS}/\Delta x < 0$ and if $q_s > 0$ (nourishment)
Erosion if $\Delta Q_{LS}/\Delta x > 0$ and if $q_s < 0$ (sand mining)
Equation (2.12) is solved by an explicit Lax-Wendorf scheme, as follows:.

$$y_{s,i\ new} = y_{s,i,old} + \Delta y_{s,I} \qquad (2.13)$$

with
$\Delta y_{s,i} = [(q_s)\,(2\Delta x) - (Q_{SL,i+1,old} - Q_{SL,i-1,old})]\,[\Delta t/(2\,h\,\Delta x)] + 0.5\,\gamma\,[y_{s,i+1,old} + y_{s,i-1,old} - 2\,y_{s,i,old}]$
γ = smoothing parameter (0.0001 to 0.001; $\gamma = 0$ = no smoothing)

2.3 Sensitivity runs

The computation of the coastline using the LONGMOR-model is dependent on the applied wave climate and the wave order. Furthermore, the computation of the coastline position involves a smoothing parameter to suppress numerical oscillations of the computed coastlines. The coastline position is numerically computed from an explicit Lax-Wendorf scheme including a smoothing-parameter. The value of the smoothing parameter (in the range of 0.0001 to 0.001) has to be determined by trial and error.

Sensitivity runs have been made for a coastal extension of 1000 m perpendicular to the coast of North-Holland (The Netherlands) as shown in **Figure 2.3.1**. The applied offshore wave climate (9 conditions) is given in **Table 2.3.1**. This schematized wave climate represents annual-averaged conditions over a period of about 8 years (1980-1988; North-Holland) and produces a net longshore transport along the coast in northern direction (from left to right in **Figures 2.3.1, 2.3.2** and **2.3.2)**. Positive wave angles yield longshore transport to the right.
To evaluate the effect of the wave order, the waves of **Table 2.3.1** have been applied in:

- positive-negative order; all waves with positive wave angles are taken first;
- negative-positive order (reversed order); all waves with negative wave angles are taken first*;*
- alternating order; waves with alternating positive and negative angles.

Time (days)	Significant wave height at deep water $H_{s,o}$ (m)	Peak wave period T_p (s)	Angle wave direction at deep water to coast normal (degrees)
0	1.5	4.9	58
44	1.5	4.9	58
44.1	1.8	5.4	28
87	1.8	5.4	28
87.1	2.75	6.6	28
102	2.75	6.6	28
102.1	2.0	5.7	-2
128	2.0	5.7	-2
128.1	1.8	5.4	-32
155	1.8	5.4	-32
155.1	1.6	5.1	-32
181	1.6	5.1	-32
181.1	3.0	6.9	-2
189	3.0	6.9	-2
189.1	3.2	7.2	-32
191	3.2	7.2	-32
191.1	0.5 m (no wind)	0.5	5.
365	0.5 m (no wind)	0.5	5.

Table 2.3.1 *Schematized annual wave climate (9 conditions) of the North-Holland coast (1980-1988)*

Figure 2.3.1 shows computed coastlines for a coastal extension of 1000 m and a net longshore transport of 500,000 m^3/year based on waves in positive-negative order. Positive wave angles yield longshore transport to the right. The grid size is 50 m and the time step is 0.005 day (432 s). The numerical oscillations are relatively large if the smoothing = 0. The oscillations can be suppressed by using smoothing= 0.0005 and 0.001. The computed coastline is asymmetric, which is in agreement with the net longshore transport to the right. Using a smoothing= 0.0005, stable, but inaccurate results are obtained. The asymmetry of the computed coastline is suppressed.

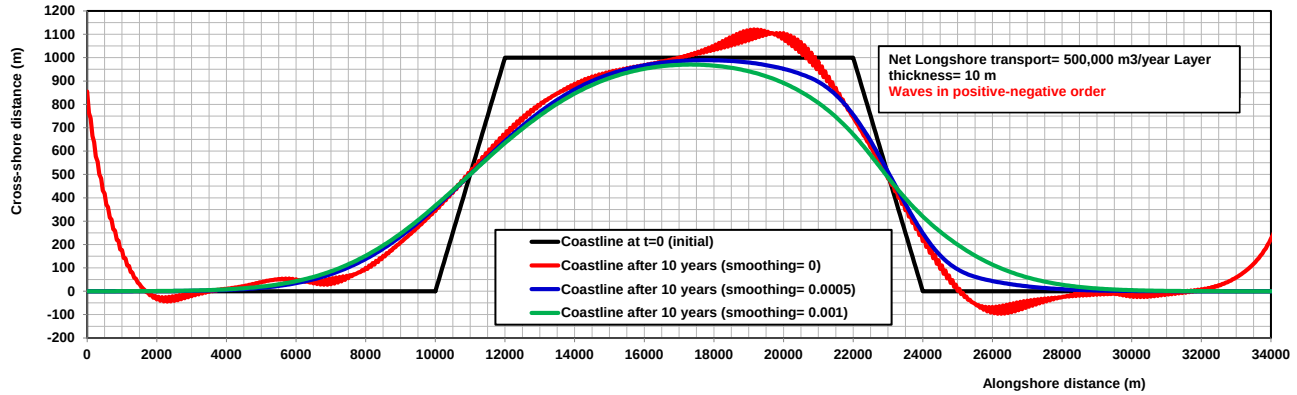

Figure 2.3.1 *Coastlines; effect of wave order and smoothing parameter; positive-negative wave order*

Figure 2.3.2 shows computed coastlines for a coastal extension of 1000 m and a net longshore transport of 500,000 m^3/year based on waves in (reversed) negative-positive order. The numerical oscillations are relatively large if the smoothing = 0. The oscillations can be suppressed by using smoothing= 0.001. As a result, the computed erosion (total erosion area) increases by about 5%.

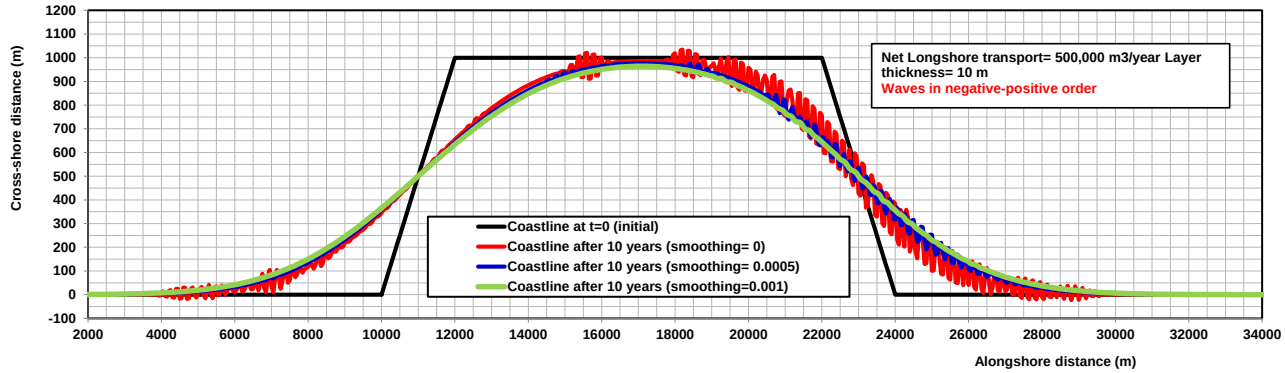

Figure 2.3.2 *Coastlines; effect of wave order and smoothing parameter; negative-positive wave order*

Figure 2.3.3 shows computed coastlines for a coastal extension of 1000 m and a net longshore transport of 500,000 m^3/year based on waves in alternating order (alternating positive and negative wave angles). The numerical oscillations are absent for smoothing = 0. Minor instabilities are present at the boundary x=0, which can be suppressed by very minor smoothing =0.00003. Both coastlines lines are very close. The computed coastline after 10 years is slightly asymmetric.
These test computations show that for numerical stability it is best to apply a wave table with waves in alternating order (alternating positive and negative wave angles). The wave order slightly influences the accuracy of the long term coastline position (suppression of asymmetry). A smoothing parameter equal to 0.00003 introduces an erosion inaccuracy < 3%.

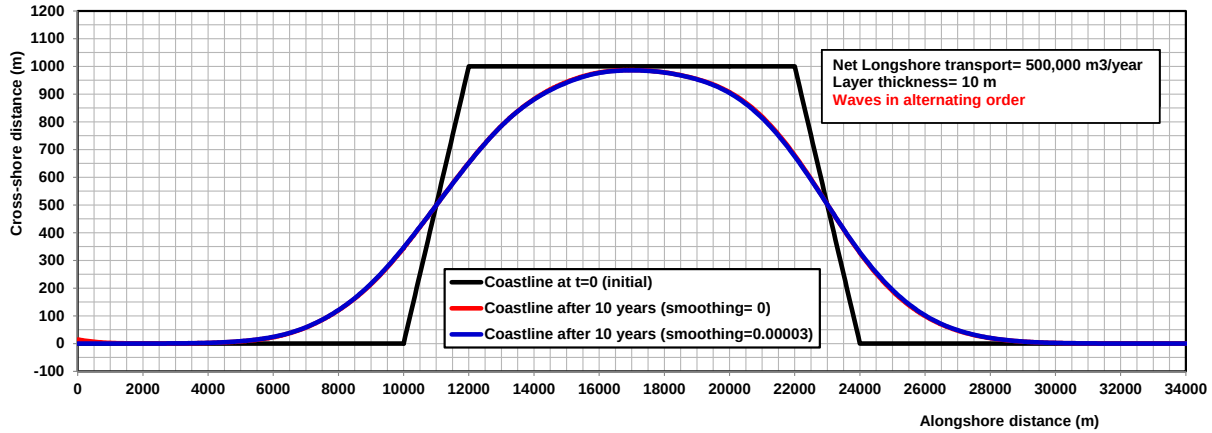

Figure 2.3.3 *Coastlines; effect of wave order and smoothing parameter; alternating wave order*

3. Application cases

3.1. Coastline changes south of IJmuiden, North-Holland, The Netherlands

The LONGMOR-model has been used to compute the coastline changes south of the harbor breakwaters at IJmuiden (**Figure 3.1.1**), The Netherlands.
The input parameters are:

- wave climate, see **Table 3.1.1** (only waves from south-west directions; data period 1979-2009);
- sediment properties: d_{50}=0.0002 m, d_{90}=0.0003 m;
- beach slope tanβ =0.01;
- breaking coefficient γ=0.6;
- effective tidal velocity=0.2 m/s (to north);
- grid size= 50 m; time step= 0.1 days; total time duration=40 years;
- initial coastline profile at 1965;
- shore normal at IJmuiden to North =104 degrees.

Significant wave height at deep water (m)	**Wave period at deep water (s)**	**Wave direction at deep water to north (°)**	**Wave direction at deep water to coast normal (°)**	**Duration (days)**
0.6	4.7	40	-64	**11**
0.6	4.7	95	-9	**16**
0.85	5.2	40	-64	**29**
0.85	5.2	95	-9	**15**
1.15	5.7	35	-69	**23**
1.32	5.7	90	-14	**18**
1.3	5.7	20	-84	**1.5**
1.7	5.7	45	-59	**23**
1.7	5.7	95	-9	**9.4**
1.9	7	45	-59	**14.7**
1.9	7	95	-9	**7.6**
2.5	7	45	-59	**8.7**
2.5	7	95	-9	**4.6**
2.9	8.4	45	-59	**4.2**
2.9	8.4	95	-9	**2.8**
3.2	8.4	45	-59	**1.8**
3.2	8.4	95	-9	**1.6**
3.6	8.4	45	-59	**0.6**
3.6	8.4	95	-9	**1.0**
4.5	9.3	45	-59	**0.2**
4.5	9.3	95	-9	**0.5**
5.0	9.3	45	-59	**0.1**
5.0	9.3	70	-34	**0.1**
5.5	10.2	95	-9	**0.1**
				total=194.5 days

Table 3.1.1 *Wave climate IJmuiden, The Netherlands*

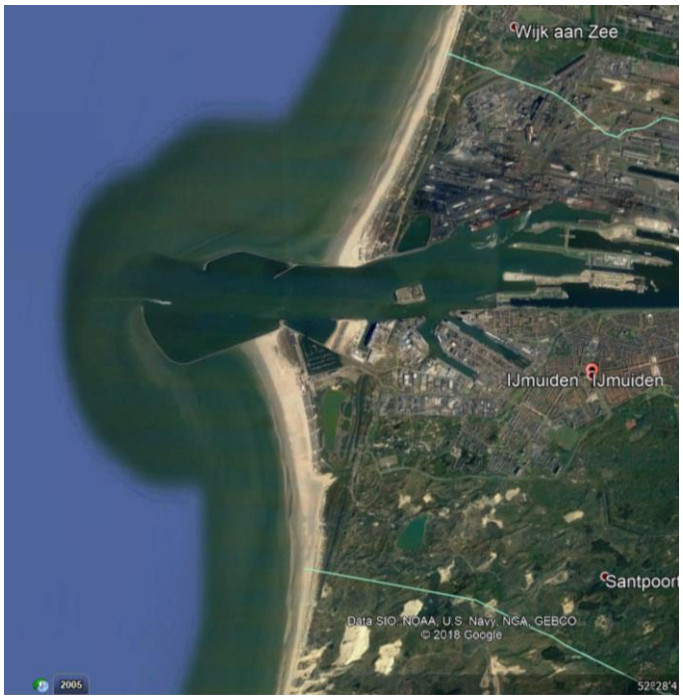

Figure 3.1.1 *Coastal accretion south of IJmuiden, The Netherlands*

Longshore transport Van Rijn (2014):
Two sediment diameters have been used d_{50}=0.2 mm and d_{50}=0.25 mm
Two calibration factors have been used K=0.5 and K=1.
Using d_{50}=0.2 mm and K=1 the measured coastline is overpredicted, see **Figure 3.1.2**.
The best results are obtained for K = 0.5.

Longshore transport Kamphuis (1991):
Using d_{50}=0.2 mm and K=1, the coastline is underpredicted, see **Figure 3.1.2**.

The annual longshore transport is (only waves from south-west based on **Table 3.1.1**):

Van Rijn	d_{50}=0.2 mm	K=1:	Q_L=740000 m^3/year
		K=0.5:	Q_L=370000 m^3/year
	d_{50}=0.25mm	K=1:	Q_L=600000 m^3/year
		K=0.5:	Q_L=300000 m^3/year
Kamphuis	d_{50}=0.2 mm	K=1:	Q_L=220000 m^3/year

Based on this, the net longshore transport going to the North is of the order of 300,000 to 370.000 m³ per year.

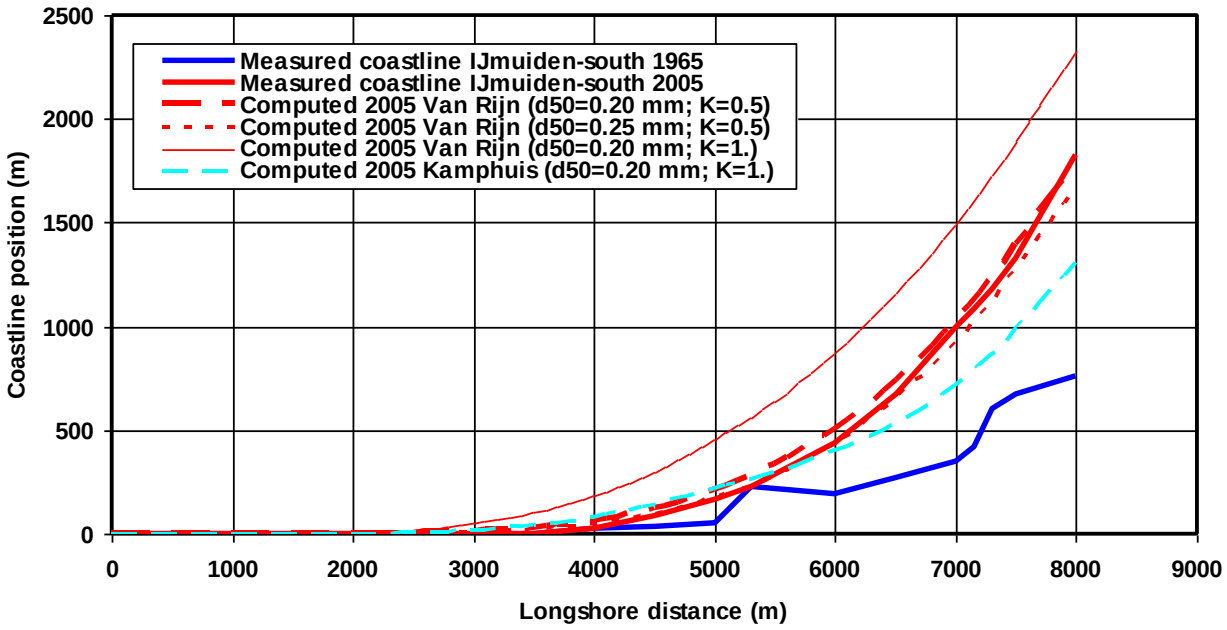

Figure 3.1.2 *Measured and computed coastlines south of IJmuiden, The Netherlands*

3.2 Coastline changes at mega-nourishment of Sand-motor, South-Holland, The Netherlands

The LONGMOR-model has been used to simulate the observed coastline changes and erosion volumes of the 'sand-motor' Case (**Figure 3.2.1**). This Case represents the dumping of a large volume of sand (about 20 million m^3) at coast south of The Hague in The Netherlands. The project is known as the sand motor. The net longshore transport of sand (d_{50}= 0.21 mm) in the situation without 'sand-motor' is assumed to be about 200,000 m^3/year based on earlier analysis results.

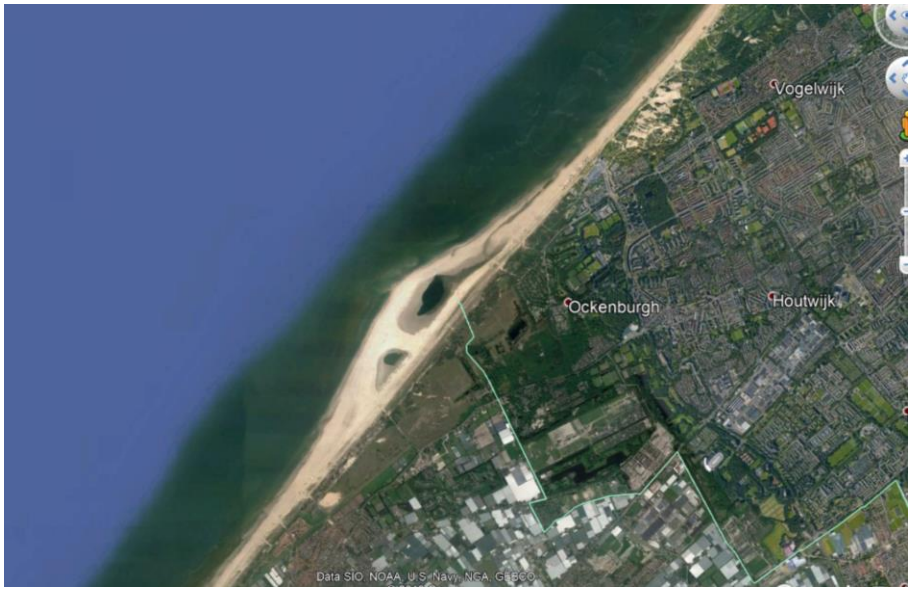

Figure 3.2.1 *Coastal extension/mega-nourishment at the coast south of the Hague, The Netherlands*

PARAMETER	Values
Grid size and length	50 m; 12.5 km
Timestep	0.002 day
Grid-'smoothing'	0.00001
Sand d_{50} and d_{90}	0.21 mm; 0.5 mm
Slope surf zone 0 to -7 m NAP	1 to 100
Breaker coefficient	0.6
Wave order	Alternating (positive and negative angles)
Layer thickness of active zone	10 m (between -7 m and +3 m NAP)
Longshore transport formula	Van Rijn (2014)
File name	zandm1.inp; zandm2.inp

Table 3.2.1 *Model settings LONGMOR for 'sand-motor', South-Holland*

The model settings are given in **Table 3.2.1.** Three offshore wave climates have been used, see **Tables 3.2.2, 3.2.3, 3.2.4** and **3.2.5**. The most detailed wave climate consists of 34 wave conditions (wave angles between 60° and -60° to the normal line to the original coast) based on wave measurements in the period 1980-1988 at an offshore depth of 30 m. Onshore-directed waves > 0.5 m are only present during 108 days. The other climates consist of schematized wave conditions with 9 and 10 conditions.
The longshore sand transport equation of Van Rijn 2014 has been used.

Figure 3.2.2 shows the computed net longshore transport rates after 1 year using various wave climate conditions. The net longshore transport rate at the updrift boundary of the model is about 200,000 m^3/year. The LONGMOR-model has also been used in combination with a very simple wave climate consisting of four wave conditions. This wave climate was calibrated to give an erosion volume of about 1.1 million m^3 after 1 year (see **Figure 3.2.3**) and a net longshore transport of 200,000 m^3/year at the updrift boundary. It is essential to include waves from almost normal directions to the coast, as these waves yield the largest erosion at the flanks of the coastal extension (nourishment).
The maximum transport gradient averaged over 1 year is approximately:

- 0.8 million m^3/year based on 10 wave conditions,
- 0.5 million m^3 based on the detailed wave climate with 34 conditions,
- 1.1 million m^3/year based on the calibrated wave climate with 9 conditions,
- 1.1 million m^3/year based on the simple wave climate with 4 conditions.

Sensitivity computations using other model settings yield a variation range of about 0.15 million m^3/year. The computed erosion volumes of 0.5, 0.8 and 1.1 million m^3 after 1 year are considerably smaller (factor 1.5 to 3) than the measured value of 1.5 million m^3.

The computed coastline recession after 1 year based on wave climate with 9 conditions is shown in **Figure 3.2.2**. The computed average coastline recession between x= 5300 m and x= 7000 m is about 60 m. The average 'measured' coastline recession over the length of the central section (x=5300 m to 7300 m; layer thickness= 10 m) of the 'sand-motor' is 1.500,000/(10x2000) = 75 m (**green dotted line**). The measured coastline after 1 year (coastline=waterline= 0 m NAP; **green dashed line**) is situated far more landward than the measured average recession line, which points to relatively large erosion near the waterline.
It is concluded that the 1D-LONGMOR-model can be used to compute the coastline changes, provided that some measured coastline data are available for calibration.

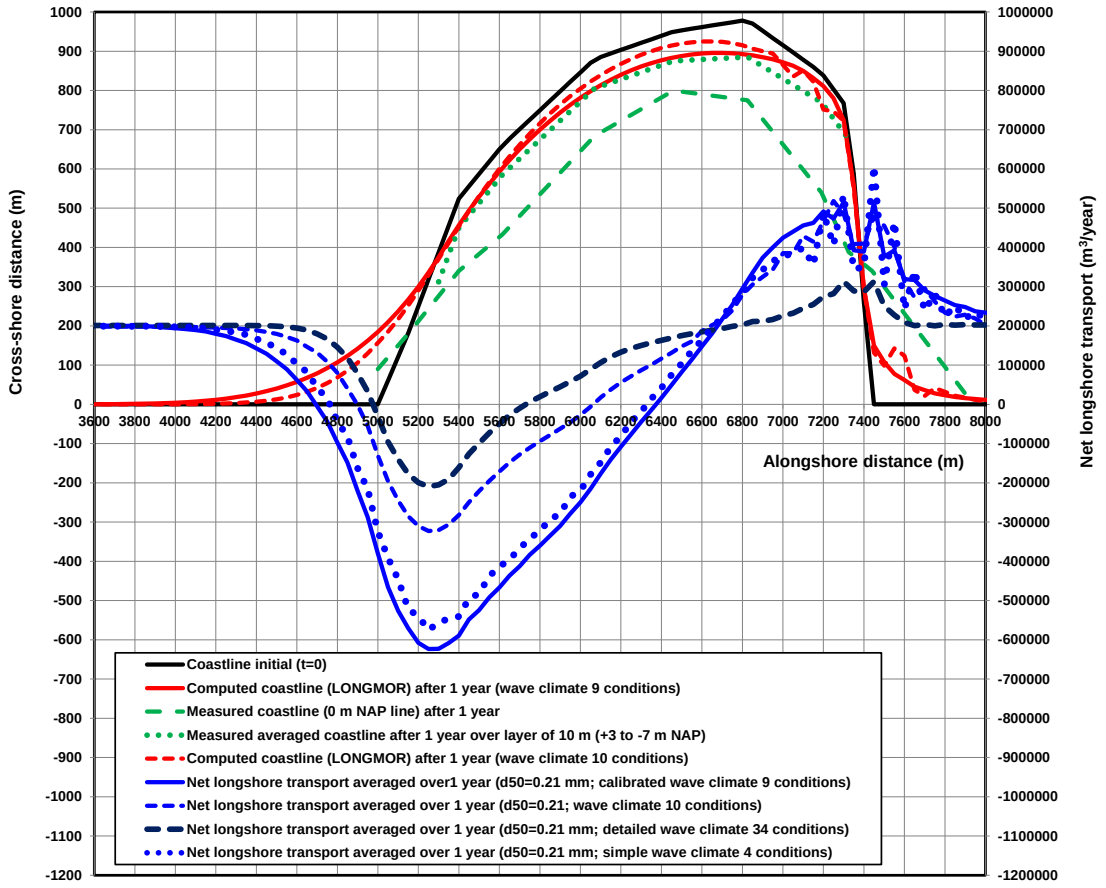

Figure 3.2.2 *Computed longshore transport rates;*
Computed and measured coastlines after 1 year, 'sandmotor', The Netherlands

Figure 3.2.3 shows the computed erosion volumes of the 1D-model based on four different wave climates. The measured initial erosion volumes after 0.5 and 1 year are significantly underestimated using a detailed wave climate with 34 conditions. These results show the strong effect of the wave climate on the 1D-model results. The 1D model underestimates the measured erosion volumes significantly using this detailed wave climate. The results of the 1D-model can only be improved by calibration of the wave climate (adjusting the wave angles and the durations) using measured erosion volumes.

The detailed DELFT3D-model yields an erosion volume of 3 million m³ after 3 years based on a wave climate with 10 conditions. The LONGMOR-model run with the same 10 wave conditions yields an erosion volume of about 2.5 million m³ after 3 years (30% less).
The discrepancies between the DELFT3D and the LONGMOR-results are caused by the following effects:

- different wave refraction seaward of the active surf zone (depth contours outside surf zone are almost stationary in Delft3D-model whereas they are rotating in LONGMOR-model similar as the coastline rotation);
- flow contraction resulting in an increase of the tide-driven velocities and transport rates (neglected in LONGMOR);
- wave focusing resulting in enhanced wave heights at both seaward corners (neglected in LONGMOR);
- erosion due to cross-shore transport gradients which may be relatively large during the initial years due to the presence of relatively steep beach profiles (neglected in LONGMOR).

The 1D-LONGMOR-model can be calibrated to better represent the measured values by adjusting the wave conditions slightly (9 conditions).

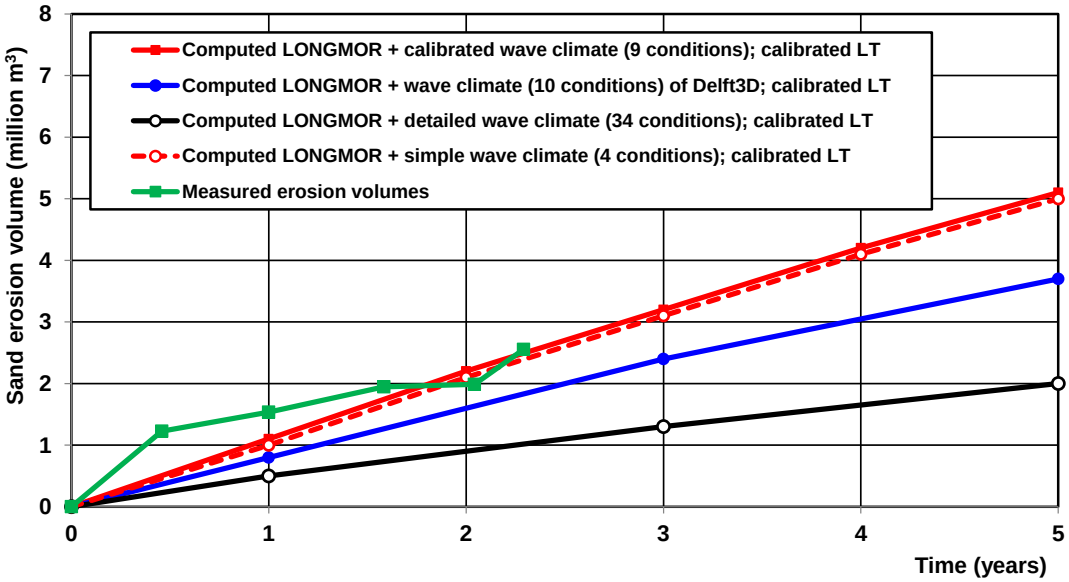

Figure 3.2.3 *Measured and computed LONGMOR erosion volumes, sand-motor, The Netherlands*

TIme (days)	Significant wave height at deep water $H_{s,o}$ (m)	Peak wave period T_p (s)	Angle wave direction at deep water to coast normal (degrees)
0	1.08	5.2	58
71	1.08	5.2	58
71.1	2.43	6.9	56.6
82.	2.43	6.9	56.6
82.1	0.89	5.2	30.3
141.	0.89	5.2	30.3
141.1	2.64	7.2	30.4
149.	2.64	7.2	30.4
149.1	0.84	5.7	-1.5
212.	0.84	5.7	-1.5
212.1	0.72	5.2	-58.3
263.	0.72	5.2	-58.3
263.1	2.61	7.5	-1.6
270.	2.61	7.5	-1.6
270.1	0.82	5.9	-30.3
356.	0.82	5.9	-30.3
356.1	2.64	7.9	-25.4
364.	2.64	7.9	-25.4
364.1	2.24	7.0	-55
365.	2.24	7.0	-55

Table 3.2.2 *Schematized annual wave climate (10 conditions) of the Dutch coast*

TIme (days)	Significant wave height at deep water $H_{s,o}$ (m)	Peak wave period T_p (s)	Angle wave direction at deep water to coast normal (degrees)
0	1.5	4.9	58
44	1.5	4.9	58
44.1	1.8	5.4	28
87	1.8	5.4	28
87.1	2.75	6.6	28
102	2.75	6.6	28
102.1	2.0	5.7	-2
128	2.0	5.7	-2
128.1	1.8	5.4	-32
155	1.8	5.4	-32
155.1	1.6	5.1	-32
181	1.6	5.1	-32
181.1	3.0	6.9	-2
189	3.0	6.9	-2
189.1	3.2	7.2	-32
191	3.2	7.2	-32
191.1	0.5 m (no wind)	0.5	5.
365	0.5 m (no wind)	0.5	5.

Table 3.2.3 *Schematized annual wave climate (9 conditions) of the North-Holland coast (1980-1988)*

Significant wave height H_s (m)	Peak wave period T_p (s)	Wave direction to shore normal θ (°)	Duration (days)	Significant wave height H_s (m)	Peak wave period T_p (s)	Wave direction to shore normal θ (°)	Duration (days)
0.75	5	-60	9.7	2.75	7	-60	0.3
		60	11.8			60	2.0
		30	9.1			30	2.0
		-30	8.9			-30	1.1
1.25	6	-60	6.2	3.25	8	-60	0.1
		60	10.4			60	0.9
		30	7.4			30	1.1
		-30	6.4			-30	0.4
1.75	7	-60	2.2	3.75	8	-60	0.04
		60	6.9			60	0.4
		30	5.3			30	0.9
		-30	3.5			-30	0.1
2.25	7	-60	0.4	4.25	9	60	0.2
		60	3.4			30	0.4
		30	3.4			-30	0.07
		-30	1.7	5.0	10	60	0.1
						30	0.4
						-30	0.1
Total			97 days				11 days
							108 days

Positive wave angle yields transport to north-east (dominant longshore transport direction)

Table 3.2.4 *Detailed annual wave climate (34 conditions) of South-Holland coast 1980-1988, The Netherlands*

TIme (days)	Significant wave height at deep water $H_{s,o}$ (m)	Peak wave period T_p (s)	Angle wave direction at deep water to coast normal (degrees)
0	2.2	7.0	30
50.	2.2	7.0	30
50.1	2.0	6.0	-30
100.	2.0	6.0	-30
100.1	1.8	6.0	0.
130.	1.8	6.0	0.
130.1	0.5	4.0	0.
365.	0.5	4.0	0.

Table 3.2.5 *Simple annual wave climate; 4 conditions; South-Holland coast 1980-1988, The Netherlands*

3.3 Coastline changes west of jetties of Port of Lagos, Nigeria

The LONGMOR-model has been used to simulate the coastline changes over a period of 50 years (1960 to 2010) for the Lagos coast updrift of the western harbor breakwater, Nigeria (**Figure 3.3.1**).
The net longshore transport at the open coast far updrift of the harbor breakwater is estimated to be about 500,000 ± 100,000 m^3/year from West to East based on analysis of old maps and charts.

To simplify the wave climate, a single offshore wave height has been used. A single offshore wave height of $H_{s,o}$= 3 m with a wave incidence angle of 30^o degrees and duration of 25 days per year yields a longshore transport of about 500,000 m^3/year (Van Rijn 2014).

The model input data of the LONGMOR-model contains various uncertain parameters, as follows:

- parameters of net longshore transport of 500,000 m^3/year (range of 400,000 to 600,000 m^3/year);
- effective profile layer thickness (range of 8 m for short term computations to 12 m for long term computations); the layer thickness is the vertical distance between the sea bottom at the breaker line at about -7 m below MSL and the dune crest at +3m above MSL (MSL= Mean Sea Level);
- adjustment length scale of longshore transport (order of 5 km); alongshore distance over which the longshore transport reduces to zero close to the breakwater;
- bypassing rate of longshore transport at tip of harbor breakwater (10% to 30% of updrift value).

Figure 3.3.1 *Lagos coast 2006, Nigeria*

Figure 3.3.2 shows the computed coastline changes along the west coast for a period of 50 years (1960 to 2010). The net updrift longshore transport has been varied in the range of 400,000 to 600,000 m^3/year. The layer thickness has been varied in the range of 10 to 12 m. The bypassing rate at the tip of the breakwater is set to 20% of the updrift value. The adjustment length is set to 5 km. Measured values of the coastline in 2010 are also shown. The LONGMOR-model produces very reasonable results for a net longshore transport of 400000 m^3/year and layer thickness values of 10 to 12 m.

The assumption of a bypassing rate of 20% of the updrift value (100,000 m^3/year) seems to be a very reasonable value. Bypassing of sand leads to deposition in the deeper entrance channel, which has to be removed by maintenance dredging. Around 2010, the western harbor breakwater has been extended with about 150 to 200 m to reduce the bypassing rate.

The cross-shore length scale of the accretion zone with respect to the original coast is about 300 m; the alongshore length scale of the accretion zone is about 9000 m. The ratio of the alongshore and cross-shore scales is about 9000/300 = 30.

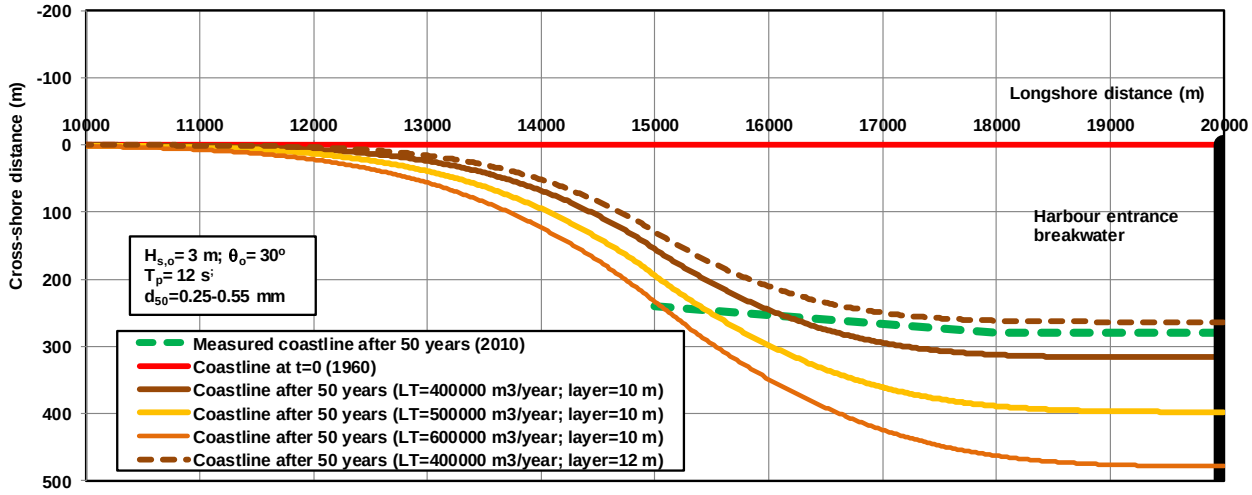

Figure 3.3.2 *Computed and measured coastline changes on west side during period 1960 to 2010, Lagos, Nigeria*

3.4 Coastline changes east of jetties of Port of Lagos in Nigeria

Approach

The coastline in the lee of a long breakwater with respect to the dominant wave direction is often suffering from erosion as result of the blocking of the longshore sand transport. An example case is the coast east of the long jetty of the Port of Lagos in Nigeria. The dominant wave direction is from the South-West.
The net annual longshore transport at the downdrift boundary should be known (input).
Most waves (about 80%) of the waves are coming from the South-West and are diffracted around the eastern breakwater of the harbor entrance, as can be seen in **Figure 3.4.1**. Wave diffraction is the lateral transfer (along the wave crest) of energy. Diffracted waves in the lee diffraction zone are smaller than the waves outside the diffraction zone. The beach of Kuramo waters has a length of about 1.6 km and the west beach end is at 2.3 km from the eastern harbor breakwater.

Two models have been used to determine the coastline changes in the lee of a breakwater:

- LONGMOR-model and;
- DWS-model (Diffracted Waves and Sand transport).

The LONGMOR-model is a state-of-the art coastline model based on longshore sand transport equations and computes the behavior of the coastline over time.
The DWS model is a simple spreadsheet model (Van Rijn 2015) to compute the wave heights, current velocities and alongshore sand transport rates along the breaker line in the wave diffraction zone of a long breakwater based on standard text-book equations of wave-diffraction processes. The computed wave heights are very close to the computed values of the very sophisticated SWAN wave-model.

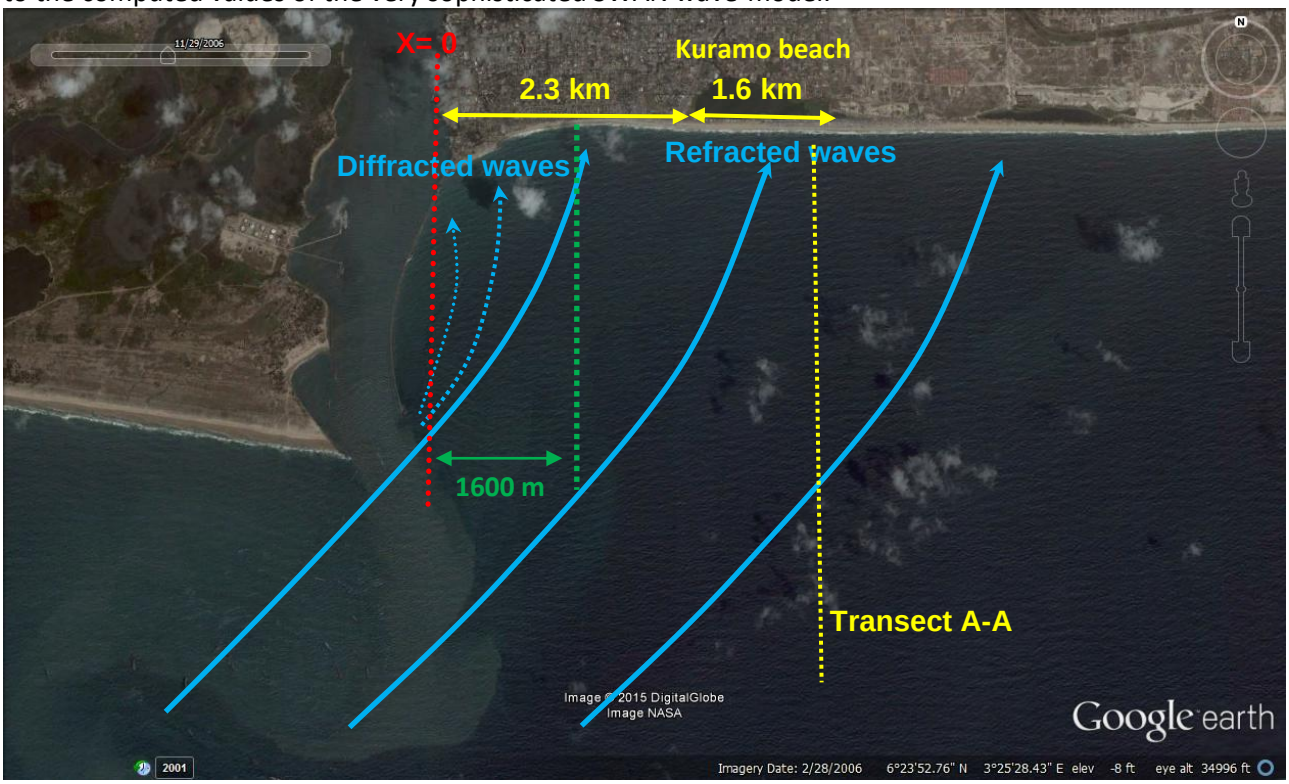

Figure 3.4.1 *Wave patterns in lee zone of eastern harbor breakwater (before 2010); waves from South-West*

Wave diffraction modelling

The DWS-model, which is based on the practical diffraction method of Kamphuis (1992), has been used to estimate the wave heights along the nearshore breaker line in the wave diffraction zone near Kuramo beach for a storm event with offshore wave height $H_{s,o}$= 4 m, T_p= 15 s and offshore wave angle of 30° from South-West (see **Table 3.4.1**). It is noted that this method is most valid for irregular directional waves and does not predict the (theoretical) wave height increase which may occur in the divergence zone.

Parameters	**Storm 1**	**Storm 2**	**Storm 3**
Offshore significant wave height (m)	2	3	4
Offshore wave angle to shore normal (°)	30	30	30
Peak wave period (s)	10	12	15
Nearshore circulation current in surf zone towards breakwater (m/s)	-0.3	-0.4	-0.5
Tidal current velocity in surf zone far downdrift away from breakwater (m/s)	0.1	0.1	0.1
Offshore water depth (m)	100		
Water depth near tip of breakwater	7		
Distance of tip of breakwater from shoreline (m)	2800		
Distance of offshore location from shoreline (m)	20000		
Slope surf zone (tan)	0.015		
Breaker coefficient γ_{br} (-)	0.6		
Friction factor f_w (-)	0.01		

Table 3.4.1 *Input data DWS-model; no land reclamation; waves from South-West*

Figure 3.4.2 shows the computed significant wave heights and wave angles at the breaker line of Kuramo beach and surrounding coastlines for the situation without land reclamation based on the DWS-model; the wave breaking coefficient is γ_{br} = 0.6. The origin x=0 is the red line through the tip of the eastern breakwater, see **Figure 3.4.1**. The longshore current velocity is also shown (+ to East; - = to West). The breaker line is at about 6.5 m depth for offshore waves of $H_{s,o}$= 4 m.

The beach of Kuramo waters is between x=2.3 and 3.9 km from the entrance breakwater, see **Figure 3.4.1**. The wave diffraction zone with reduced wave heights has an alongshore length of about 3 km. Outside the wave diffraction zone (x>3000 m), the wave height is approximately constant. The wave height at x=0 is about 65% of the wave height outside the wave diffraction zone. The wave angles at the breaker line are about 10° (waves almost normal to the shore). Bottom friction is rather important as the swell waves are relatively long waves propagating from deep water of 100 m over a distance of about 20 km to the shore (large friction distance).

The wave height at the *west* end of Kuramo beach is about 90% of the far east wave height.

The wave height at the *east* end of Kuramo beach is about equal to the far east wave height.

The longshore current velocity is negative (towards the breakwater; to the West) with a value of about -0.5 m/s close to the breakwater and positive further away from the breakwater. The transition from negative to positive velocity occurs at about 1300 to 1500 m from the harbor breakwater. The transition location marks the location of maximum erosion (which is about 1600 m from the harbor breakwater). The longshore current velocity based on the DWS-model increases gradually to about 0.7 m/s faraway from Kuramo beach for offshore waves of 3 to 4 m.

The wave height at the west end of Kuramo Waters beach is slightly smaller than at the east end of the beach. Similarly, the longshore current velocity increases slightly along Kuramo beach.

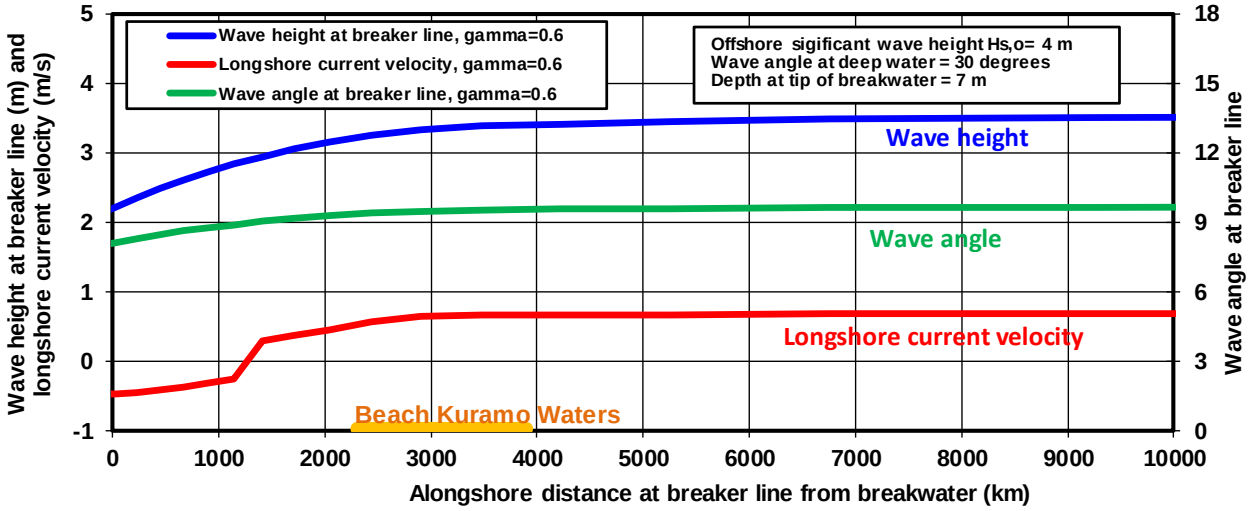

Figure 3.4.2 *Wave height and wave angle along the breaker line in the lee area of a breakwater; DWS-model; $H_{s,o}$= 4 m from South-West; γ_{br}= 0.6; (+ to East; - = to West)*

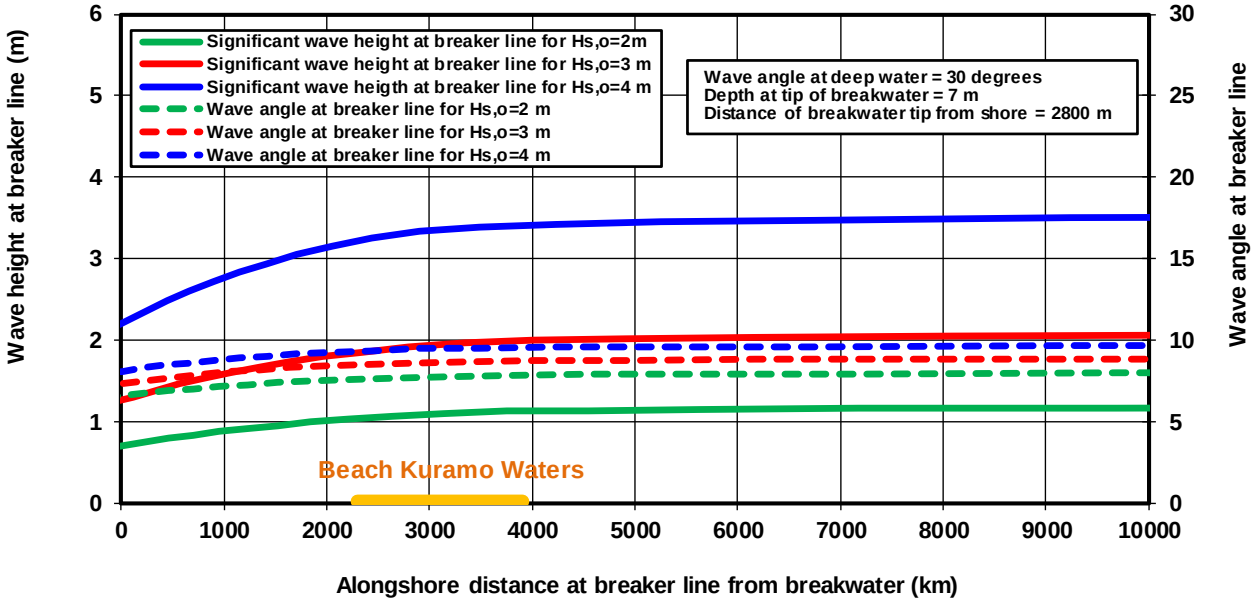

Figure 3.4.3 *Wave height and wave angle along the breaker line near Kuramo beach; DWS-model; $H_{s,o}$= 2, 3 and 4 m from South-West; γ_{br}= 0.6*

Table 3.4.2 shows the wave heights at depth lines of 7 and 5 m for Kuramo West and East based on the DWS-model (with γ_{br}=0.6) and the SWAN-model. The SWAN-model results are best and show that the largest waves (**red** and **green** values) occur at Kuramo West due to wave focusing in the region of the protruding harbor entrance. The SWAN wave height is relatively small at Kuramo East for $H_{s,o}$=3 m due to wave refraction effects resulting in a dip in the wave height distribution. The transition zone from relatively small waves in the diffraction zone to the larger waves outside the diffraction zone has an alongshore length scale of about 2 km for the SWAN-model and 3 km for the DWS-model.

Depth (m)	Offshore: $H_{s,o}$=3 m; T_p=12 s; angle=30° (210° N)				Offshore: $H_{s,o}$=4 m; T_p=15 s; angle=30° (210°N)			
	Kuramo West		Kuramo East		Kuramo West		Kuramo East	
	DWS	SWAN 2D	DWS	SWAN 2D	DWS	SWAN 2D	DWS	SWAN 2D
7	2.3	**2.6**	2.6	**2.2**	3.3	**3.2**	3.7	**3.1**
5	2.2	**2.6**	2.5	**2.2**	2.7	**3.1**	3.0	**3.0**

Table 3.4.2 *Significant wave height (in m) at Kuramo West and East; waves from South-West*

Figure 3.4.4 shows the plan view with the wave and current parameters at the beach of Kuramo Waters for a storm event with $H_{s,o}$= 4 m based on DWS-model. The wave height at the breaker line varies from $H_{s,br}$= 2.2 m at x=0 m to $H_{s,br}$= 3.4 m outside the diffraction zone (x > 3 km). Near the breakwater, the longshore current is towards the structure. At Kuramo beach, the longshore current velocity increases from 0.55 m/s to 0.7 m/s in eastward direction.

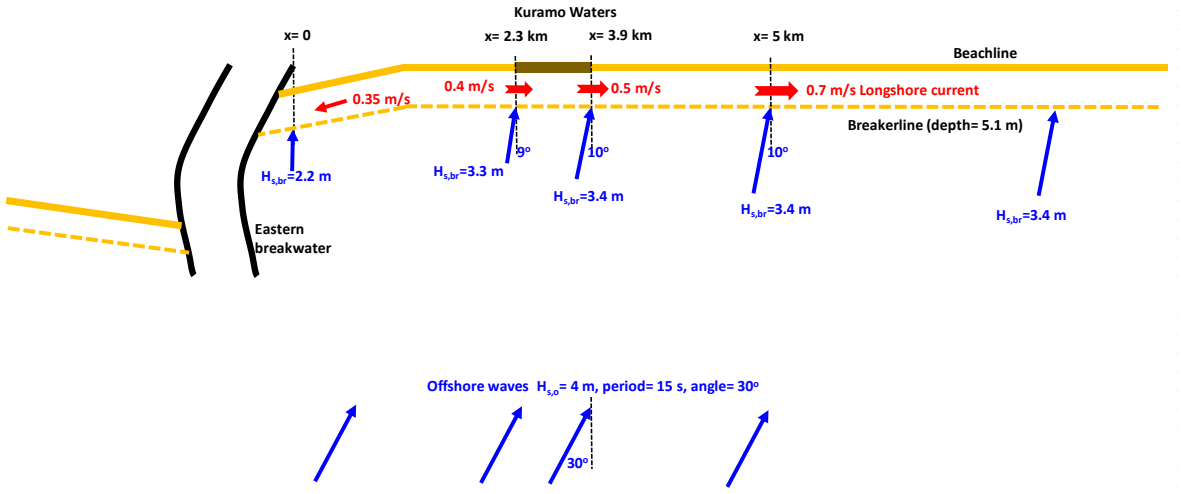

Figure 3.4.4 *Plan view for wave conditions in lee of breakwater; $H_{s,o}$= 4 m from South-West (γ_{br} = 0.6); DWS-model*

Longshore transport variations and coastline changes

To simplify the wave climate, a single offshore wave height has been used to run the LONGMOR-model.
The net longshore transport in eastern direction is about 650,000 m^3/year based on historical coastline changes for the East coast.
A single offshore wave height of $H_{s,o}$= 1.5 m with duration of 210 to 230 days per year yields a longshore transport of 650,000 m^3/year.
Similarly, a single wave height of $H_{s,o}$= 3 m yields with duration of 28 to 30 days per year also yields a longshore transport of about 650,000 m^3/year.
The LONGMOR-model has been calibrated to produce the correct distribution of the longshore transport rate at Kuramo beach and surrounding coast, as computed by the more detailed DWS-model.

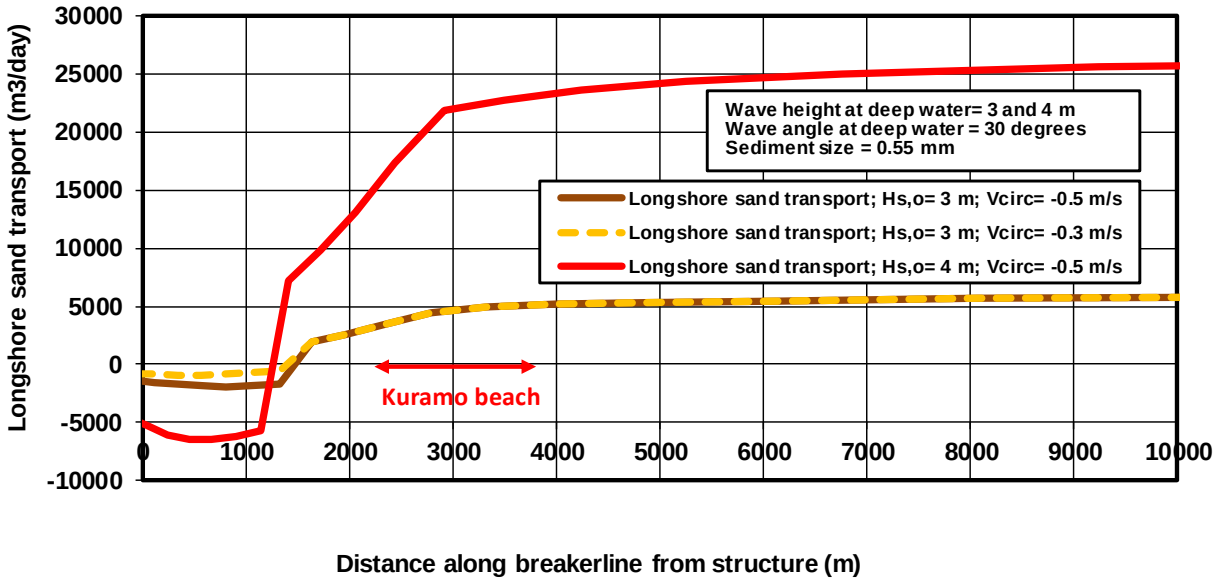

Figure 3.4.5 *Longshore transport along Kuramo beach and surrounding coastlines (DWS-model); d_{50}= 0.55 mm, $H_{s,o}$= 3 and 4 m from South-West*

Figure 3.4.5 shows the computed longshore transport of the DWS-model for $H_{s,o}$= 3 and 4 m, offshore angle= 30° (waves from South-West), d_{50}= 0.55 mm and slope= 0.015. Far away (East) from the harbor entrance channel, the longshore transport is about 6100 m³/day for offshore waves of 3 m. Using a duration of 106 days, the net longshore transport is 650,000 m³ per year.

Figure 3.4.6 shows the computed coastline of the LONGMOR-model after 5 years (2005 to 2010) for a wave climate with one wave height of $H_{s,o}$= 3 m and duration representing 5 years. The input data are given in **Table 3.4.3**. Two computations have been made, as follows:

- high estimate of the net annual longshore transport LT_{net}= 650,000 m³/year (at the far end x=15 km east of the harbor breakwater);
- low estimate of the net annual longshore transport LT_{net}= 300,000 m³/year (at the far end x=15 km east of the harbor breakwater).

The high estimate of the net LT yields coastal recession rates of 40 to 50 m after 5 years or 8 to 10 m per year at Kuramo beach, which are much too high compared with the measured data of 2 to 3 m per year.
Therefore, another computation has been made for a low estimate of the LT resulting in a recession rate of 3 to 5 m per year. The location of maximum erosion is at about 1800 to 2000 m from the harbor breakwater. The alongshore scale of the coastal erosion on the east coast is of the order of 10 km, see **Figure 3.4.6**. It is noted that the region of maximum erosion will gradually shift eastwards with the construction progress of the Lagos Wall (after 2010).
The net annual longshore transport rate to simulate the coastal recession rates at Kuramo beach before the construction of the land reclamation correctly is of the order of 300,000 m³/year, which is considerably less than the value of about 500,000 to 900,000 m³/year derived from the long term historical coastline recession rates of the East coast. Most likely, the present recession rates are smaller than the older recession rates due to the presence of local coastal defense structures (revetments and short groins are present) and local beach nourishment schemes.

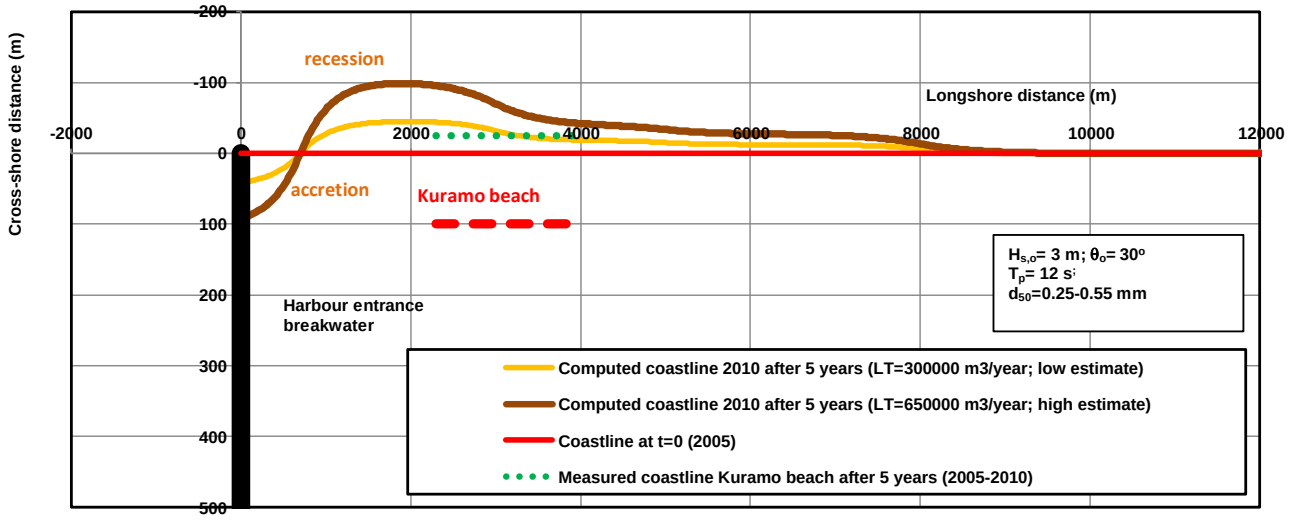

Figure 3.4.6 *Coastline along Kuramo beach and surrounding coastlines (LONGMOR-model); d_{50}= 0.25-0.55 mm, $H_{s,o}$= 3 m from South-West*

PARAMETER	VALUES
Offshore significant wave height	3 m
Offshore wave angle	30°
Peak wave period	12 s
Grid size and traject length	20 m; 15000 m
Time step and grid-'smoothing'	0.01 day; 0.01-0.5
Sand d_{50}, d_{90}	0.25-0.55 mm; 1 mm
Slope beach-surf zone 0 tot -5 m MSL	1 to 65 (tan slope=0.015)
Breaker coefficient	0.8
Layer thickness of active zone	10 m (between -8 m and +2 m MSL)
Longshore transport formula; Calibration coefficient	Van Rijn 2014; 0.45 to 1
Angle of coastnormal to North	0 degrees
Tidal currents in surf zone	V_{flood}=0 m/s; V_{ebb}=0 m/s (no effect if both values are equal)
Beach nourishment volumes	0
Input files	NigerW.inp: west coast Niger1.inp: east coast 1.4 years (Jan 2010-May 2011) Niger12.inp: east coast 2 years (May 2011-March 2013)

Table 3.4.3 *Input data of LONGMOR-model; Kuramo beach.*

3.5 Detached breakwater at 450 m from the coast in Congo

Introduction

This case refers to the design of loading facility along the coast of West-Afrika (Congo). A detached breakwater is planned to be constructed about 465 m from the shore. Between the shore and breakwater, a berthing zone will be created, see **Figure 3.5.1**.

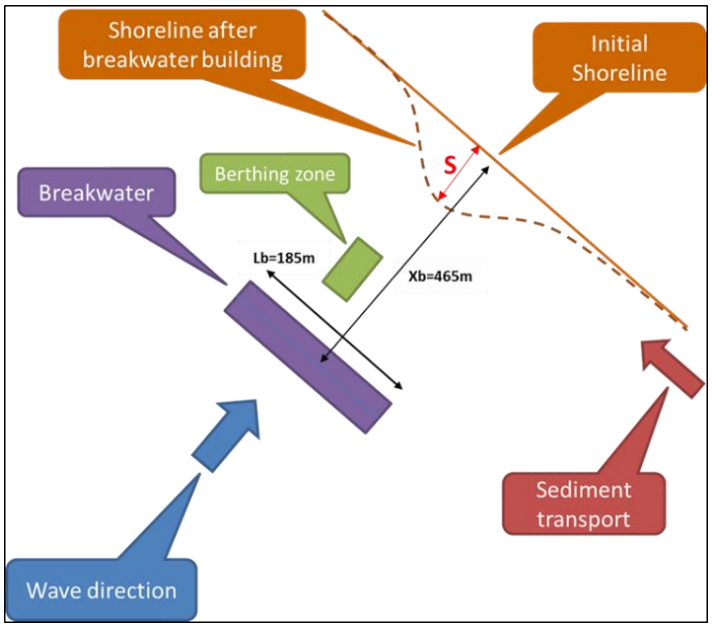

Figure 3.5.1 *Single detached breakwater*

Wave and flow patterns

The DELFT3D-flow model and the SWAN-wave model have been used to compute the wave and flow patterns and coastline changes in the lee of a (single) detached breakwater. The length of the breakwater (parallel to the coast is about 200 m. The distance between the breakwater and the coast is about 450 m.
The water depth at the position of the breakwater is about -6 m (to mean sea level).
The beach slope is 1 to 7; the surf zone slope is 1 to 20 to -6 m depth line and the sea bottom slope is 1 to 200 beyond the -6 m depth line. The beach and seabed consist of sand with d_{50}=0.3 mm and d_{90}=0.6 mm.
The representative offshore significant wave height is $H_{s,o}$=1.25 m with T_p= 12 s and a wave angle of 10° with respect to the coast normal (which makes an angle of 40° with the North, see **Figure 3.5.2**).
The net longshore transport is about 100,000 m^3/year based on Littoral.xls.

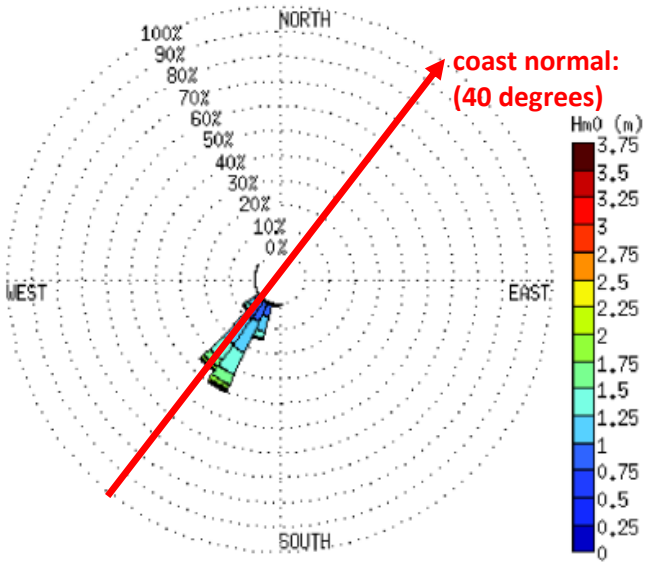

Figure 3.5.2 *Wave rose and coast normal*

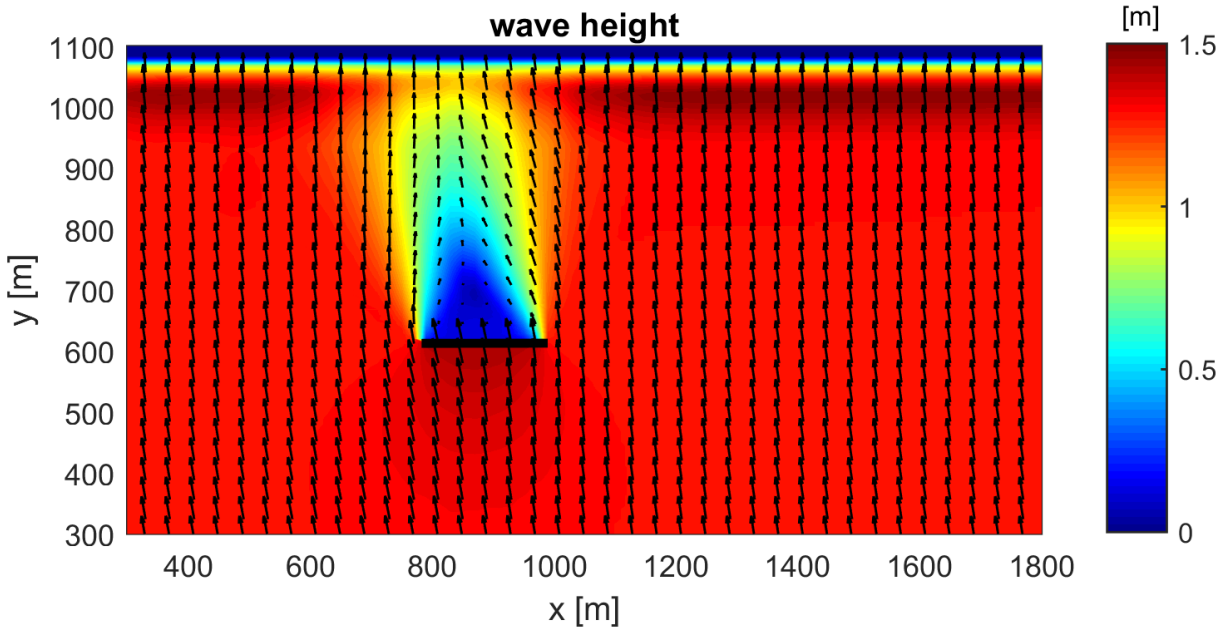

Figure 3.5.3 *Computed wave heights and directions (based on SWAN-model); $H_{s,o}$= 1.25 m*

Figure 3.5.3 shows the computed wave heights and directions in the lee of the breakwater.
The significant wave height is strongly reduced in the lee of the breakwater.

Figure 3.5.4 shows the flow velocities in the lee of the breakwater.
The wave-induced flow velocity is about 0.7 m/s at the upwave (right) side increasing to about 1 m/s in the lee of the breakwater. Circulation cells can be observed in the lee of the breakwater and at the downwave (left) side.

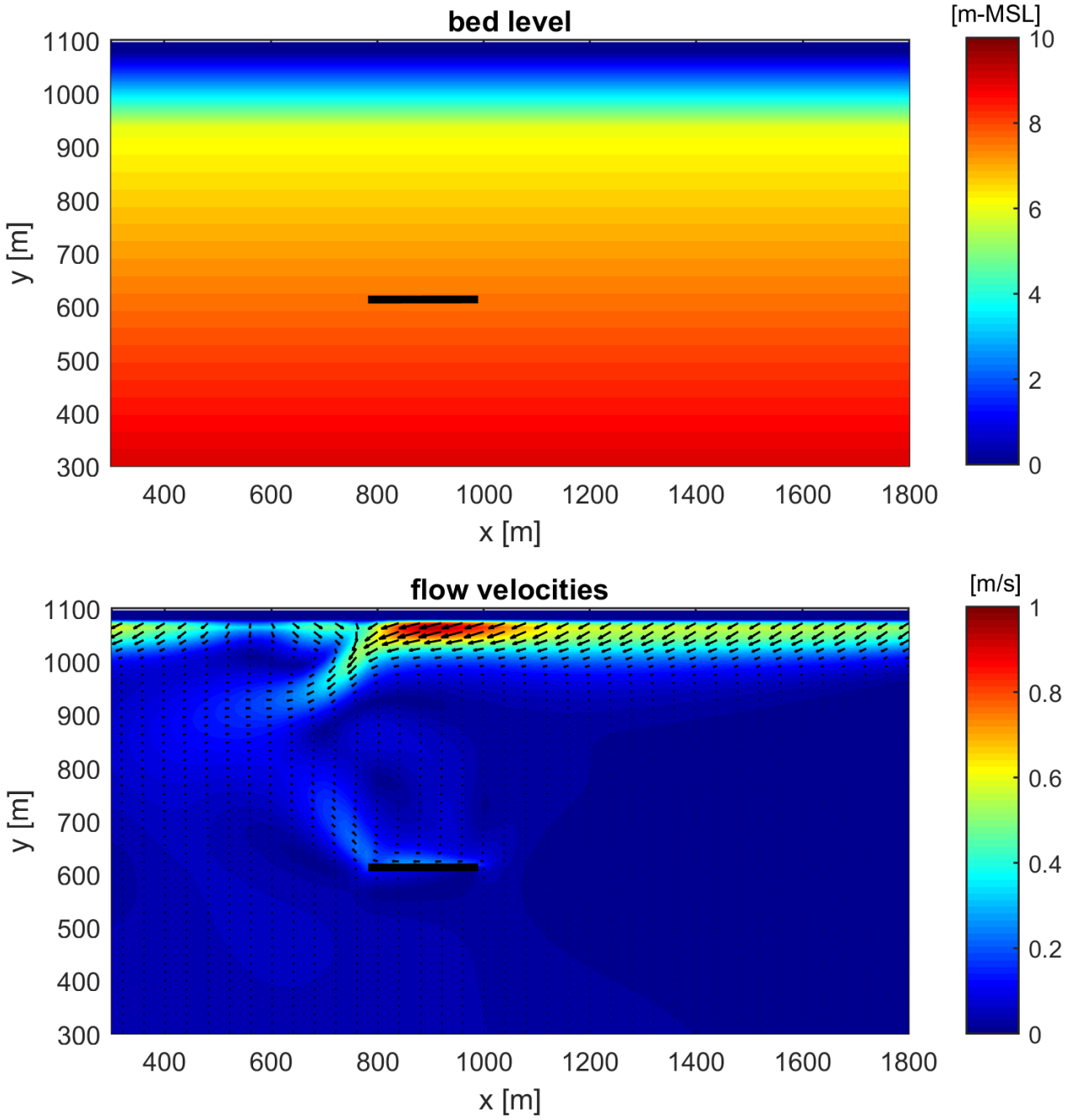

Figure 3.5.4 *Computed flow velocities (based on DELFT3D-model); $H_{s,o}$= 1.25 m*

Figure 3.5.5 shows the computed coastline changes after 5 years with the development of a salient in the lee of the breakwater.

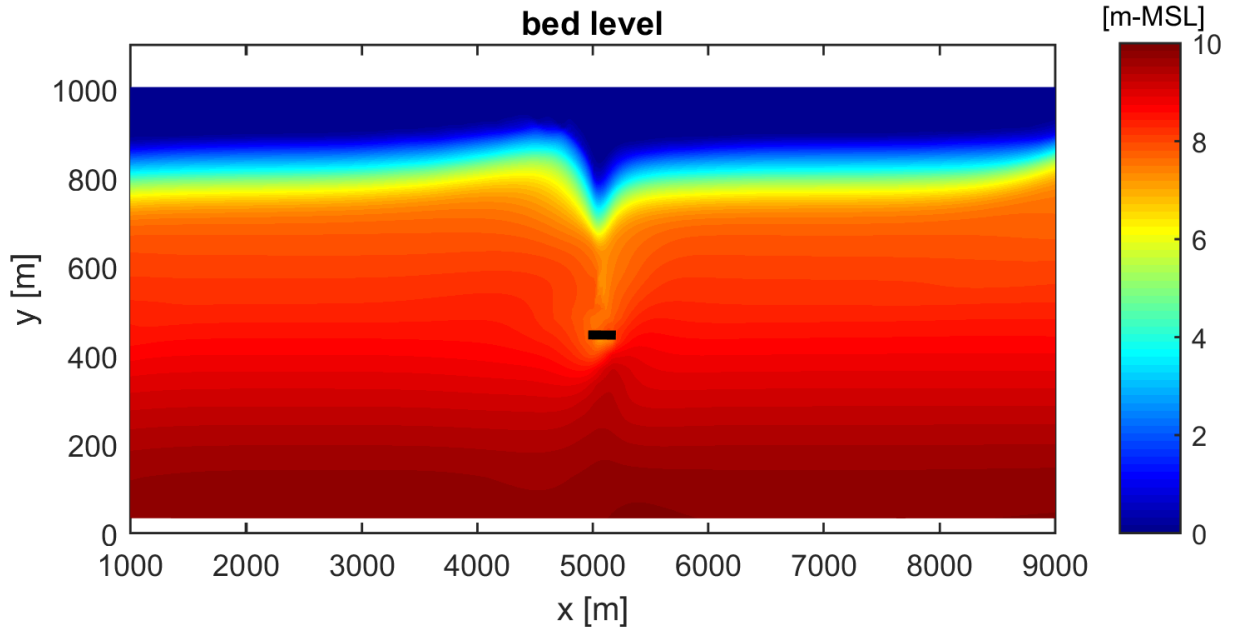

Figure 3.5.5 *Computed coastline changes (based on DELFT3D-model); $H_{s,o}$= 1.25 m*

LONGMOR-model

The LONGMOR 1D-model has been used to compute the coastline changes in the lee of the breakwater. The LONGMOR1D-model cannot accurately compute the longshore transport rates in the lee of the breakwater. Therefore, the longshore transport rates have been taken from the DELFT3D-model for one representative wave condition ($H_{s,o}$=1.25 m, T_p=12 s and wave incidence angle=10°), see **Figure 3.5.6**. These values have been used to calibrate the longshore transport rates of the LONGMOR1D-mdel.

The results of **Figure 3.5.6** shows the following phenomena:

- the longshore sand transport faraway from the structure is about 1000 m^3/day;
- the longshore sand transport increases to about 2500 m^3/day (increase of factor 2.5) in the lee of the breakwater due to the generation of circulation velocities (setup differences);
- the longshore sand transport reduces to almost nil at a distance of about 100 m downdrift of the structure due to the strong reduction in wave height and current velocity;
- the longshore sand transport increases/re-adjusts to about 1000 m^3/day over a distance of about 600 m (3 times the length of the structure) at the downdrift side.

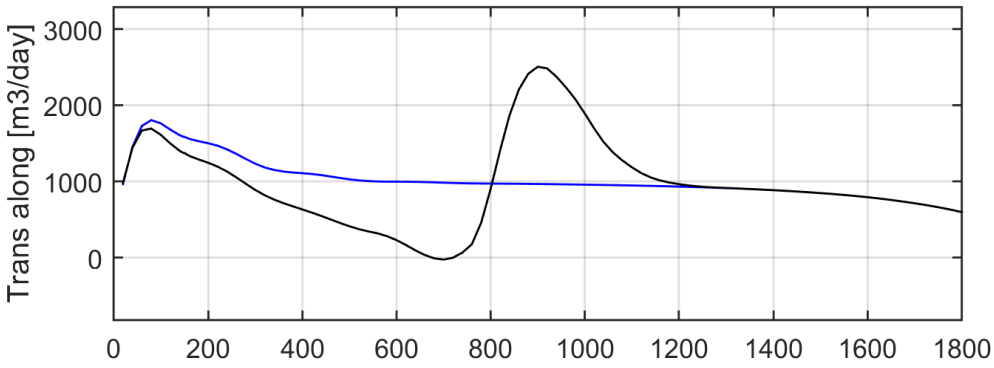

Figure 3.5.6 *Computed longshore sand transport integrated over surf zone; location structure = 800-1000 m; $H_{s,o}$=1.25 m, T_p=12 s, wave incidence angle=10^o from southwest (right)*

The input values of the LONGMOR1D-model is given in **Table 3.5.1.**

PARAMETER	VALUES
Offshore significant wave height	1.25 m during 200 days and 1.15 m during 165 days
Offshore wave angle to coast normal	10^o and -10^o
Peak wave period	12 s
Grid size and traject length	10 m; 10000 m
Time step and grid-'smoothing'	0.05 day; 0.001
Sand d_{50}, d_{90}	0.3; 0.6 mm
Slope beach-surf zone 0 tot -6 m MSL	1 to 33 (tan slope=0.03)
Breaker coefficient	0.7
Layer thickness of active zone	7 m (between +1 and -6 m to CD)
Longshore transport formula; Calibration coefficient Net longshore sand transport	Van Rijn 2014; 1.05 100,000 m^3/year
Angle of coastnormal to North	40 degrees
Tidal currents in surf zone	V_{flood}=0 m/s; V_{ebb}=0 m/s (no effect if both values are equal)
Beach nourishment volumes	0
Input files	congo1.inp;congo2.inp; congo3.inp; congo4.inp

Table 3.5.1 *Input data of LONGMOR1D-model*

The following cases have been distinguished:

- structure with 100% blocking of longshore transport;
- structure with reduced blocking (calibration based on results of DELFT3D-model);

Structure with 100% blocking

The most simple approach is to assume that the longshore sand transport is fullly blocked (blocking of 100%) by the detached breakwater (as if the breakwater acts as a groin).

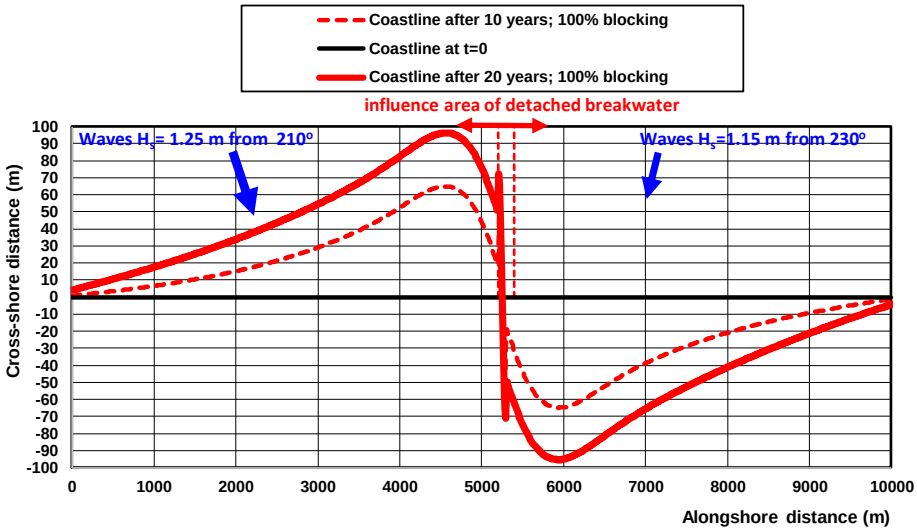

Figure 3.5.7 *Computed coastlines of LONGMOR1D-model after 10 and 20 years in the case of a structure with 100% blocking; LT=100,000 m^3/year*

Figure 3.5.7 shows the computed coastlines after 10 and 20 years. The maximum coastline accretion is about 100 m at the updrift side of the structure. The accretion extends over an updrift distance of about 5 km. Severe erosion is present at the downdrift side.

Structure with reduced blocking

A detached breakwater is a structure which allows the passage of longshore sand transport in the lee of the structure. The reduction (blocking) of the longshore sand transport depends on the ratio of the structure length (L) and the distance (D) between the structure and the coastline.

Based on the DELFT3D-model results, the LONGMOR1D-model has been calibrated to give (for both wave directions 10° and -10°):

- longshore sand transport ($Q_{LT,x=0}$) is constant up to start of breakwater;
- increase of longshore transport to $1.5Q_{LT,x=0}$ at end of breakwater;
- decrease of longshore transport to $0.2Q_{LT,x=0}$ at 200 m beyond downdrift end of breakwater;
- increase of longshore transport to $Q_{LT,x=0}$ at 400 m beyond downdrift end of breakwater;
- longshore sand transport ($Q_{LT,x=0}$) is constant up to end of computational domain.

Figure 3.5.8 shows the computed coastlines after 10, 20 and 40 years. Minimal numerical smoothing (<1%) has been applied. A salient is generated in the lee of the detached breakwater.

The maximum cross-shore extension of the salient is about 60 m after 10 years, which remains stable over a time scale of 40 years. The cross-shore extension is about 12% of the distance between the breakwater and the coast.

The alongshore length scale of the salient is about 600 to 700 m (3 times the length of the breakwater).

The coastal accretion updrift of the salient is about 15 m after 40 years; the maximum coastal recession is about 15 to 20 m on both sides of the structure after 40 years. The alongshore erosion scale is almost 3 km at the downdrift side.

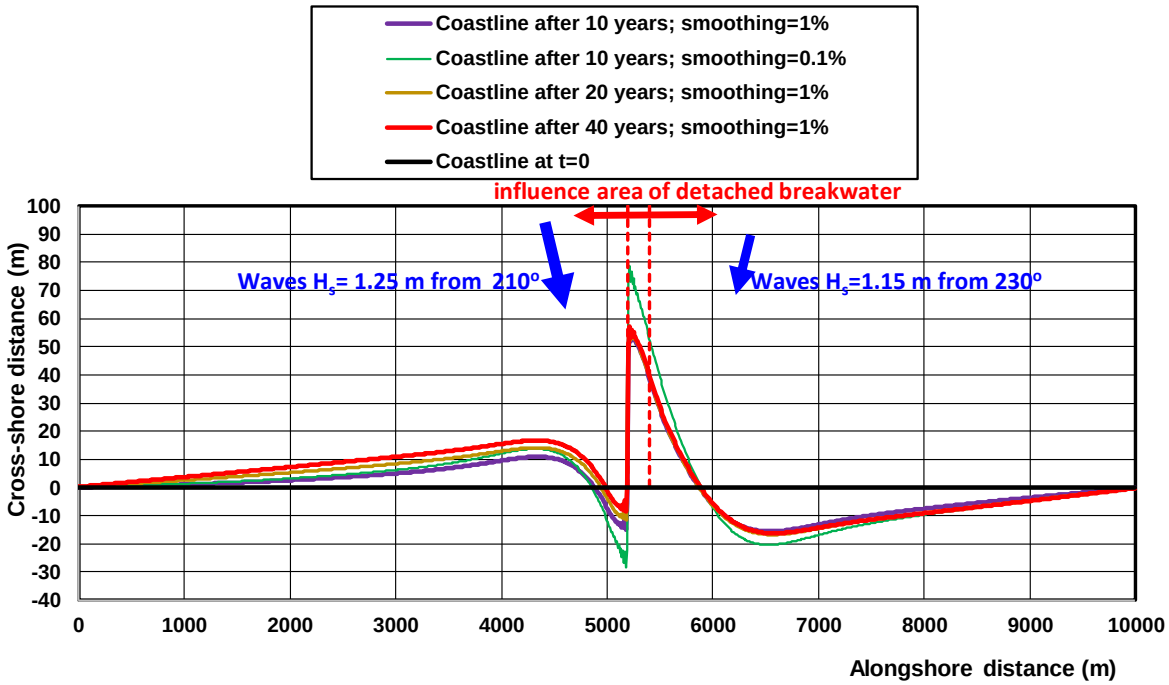

Figure 3.5.8 *Computed coastlines of LONGMOR1D-model after 10, 20 and 40 years in the case of a detached breakwater with reduced blocking; LT=100,000 m^3/year*

Figure 3.5.9 shows similar computation results for a longshore transport rate of 200,000 m^3/year (wave heights are 1.25 and 1.15 m; wave incidence angles are 20° and -20°). A much larger salient is generated in the lee of the detached breakwater. The maximum cross-shore extension of the salient is about 150 m after 40 years.
The coastal accretion updrift of the salient is about 40 m after 40 years; the maximum coastal recession is about 40 m on both sides of the structure after 40 years. The alongshore erosion scale is almost 4 km at the downdrift side.

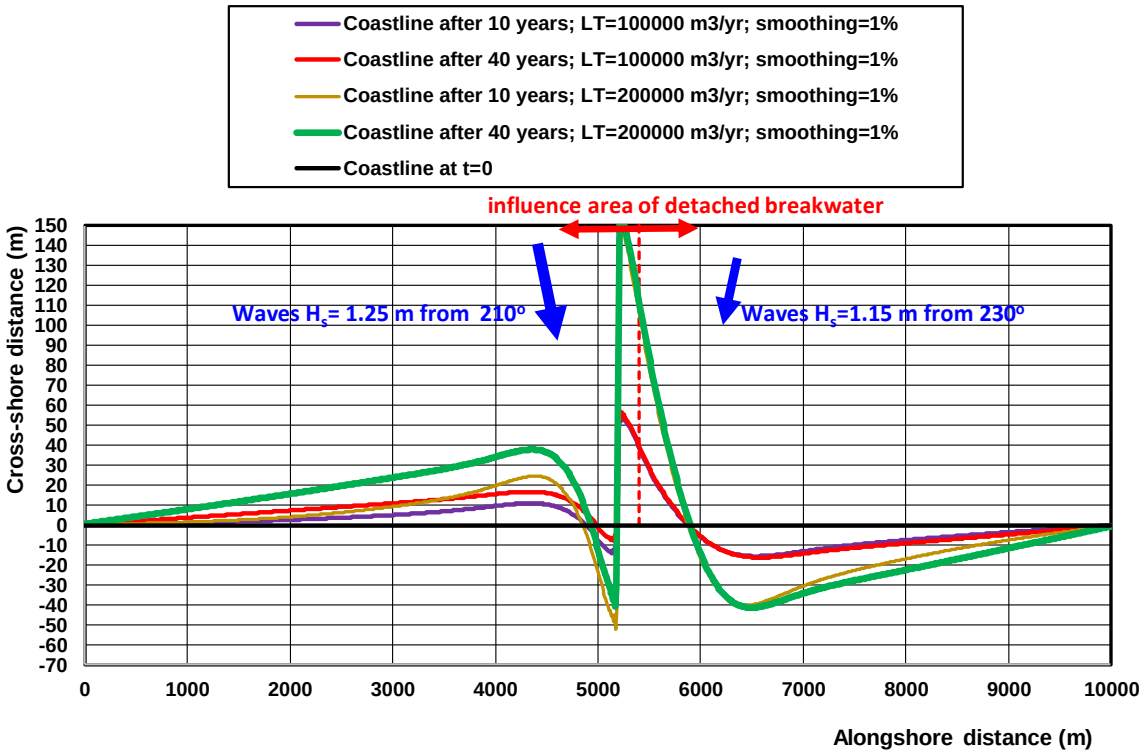

Figure 3.5.9 *Computed coastlines of LONGMOR1D-model after 10, 20 and 40 years in thecase of a detached breakwater with reduced blocking; LT=100,000 and 200,000 m^3/year*

3.6 Design of long groyne near Soulac sur Mer, France

3.6.1 General

Since long the beaches between Négade and the inlet of the Garonne in France are eroding with rates of 5 to 10 m per year despite many coastal defense works (structures). The evacuation of the building Le Signal at the beach front of Soulac in January 2014 marks the severity of the erosion problems. In response to that, Barriquand groin at the north beach of Soulac was extended in 2014 to promote more deposition of sand at the beach.
In 2018, the local authorities (Communauté de Communes Médoc Atlantigue; CDC MA) have adopted a new strategy aimed at:

- reduction of the erosion vulnerability of the coast;
- maintenance and reinforcement of defense structures at the beaches of the urbanized areas;
- regular placements of beach sand to prevent beach erosion.

The objective of the present study is to propose a series of technical coastal protection measures for the coastal section between L'Amélie and the Barriquand-groin in the north of Soulac sur Mer. This coastal section consists of (see **Figure 3.6.1**):

- Les dunes de L'Amélie (1.5 km);
- La plage des Naiades (1 km);
- Les dunes de Boulevard (0.5 km);
- La Plage centrale jusqu'a l'épi Barriquand (1 km);
- Les brise-mers des Arros, des Huttes et des Cantines (3.1 km);
- Les dunes de Tout-Vent (0.6 km).

Figure 3.6.1 *Coastal region between Point La Grave (north) and Point La Negade (south)*

3.6.2 Longshore sand transport computations

Methods

Two methods have been used to compute the longshore sand transport at various locations along the coast between Négade and Barriquand., as follows:

- simplified LONGMOR-model; which computes the wave height and the wave incidence angle at the breaker line and, based on that, the longshore sand transport rate in the surf zone for a given annual offshore wave climate; three longshore sand transport equations are implemented (CERC, Kamphuis 1991 and Van Rijn); the model is valid for uniform shorelines with shore-parallel depth contours;
- detailed CROSMOR-model; which computes the wave heights, longshore and cross-shore currents and longshore and cross-shore sand transport rates along a bottom profile normal to the shore.

The basic input parameters of both models are given in **Table 3.6.1**.

Model	Parameters	Values
LONGMOR	1. Offshore depth (m to CD)	-20
	2.Tidal currents (m/s)	0
	3. Breaking coefficient= ratio of wave height and water depth at breakerline	0.5
	3. Median sand diameter (mm)	0.35
	4. Beach slope	0.01
	5. Fluid and sediment density (kg/m^3)	1020, 2650
CROSMOR	1. Offshore depth (m to CD)	-30
	2. Depth-averaged flood/ebb tidal currents at offshore boundary (m/s)	0.3; -0.3
	3. Tidal flood/ebb water levels to mean sea level (m)	1.7; -1.7
	4. Water depth at most landward grid point (m)	0.3
	5. Storm surge level (m)	0
	6. Number of Rayleigh-distributed wave classes	10
	7. Wave breaking	automatic
	8. Horizontal mixing coefficient (m^2/s)	0.1
	9. Sand diameter d_{50}, d_{90} (mm)	0.35; 0.7
	10. Bed roughness	automatic
	11. grid size (m)	2 to 50
	12. Time step	automatic

Table 3.6.1 *General model input parameters*

LONGMOR-model results

Figure 3.6.2 and **Table 3.6.3** show the computed longshore sand transport (LST) values of Kamphuis (1991) and Van Rijn (2014) as function of the shore normal angle varied in the range of 80° to 180°. The LT-equation of Bayram et al. (2007) has also been used (see Table 3.2.1), but the values are much smaller (factor 3 to 4) than the other LT-values.

The LST-values are based on the detailed wave climate with 59 wave classes of **Table 3.6.2**.

The shore normal angle to North is defined as the angle of the normal line from the sea to the beach.

The wave incidence angle is defined as the angle of the wave propagation vector to North. Three LST-values are shown: northgoing value, southgoing value and net value.

The LST-values predicted by the method of Van Rijn are higher (up to 50%) than those of the method of Kamphuis. The method of Van Rijn (2014) has also been used with the tidal current included (depth-averaged velocity of +0.3 and -0.3 m/s in the surf zone) resulting in much smaller net northgoing longshore sand transport values (compare red solid curve and dashed red curve) as the southgoing longshore sand transport is much higher due the southgoing tidal current.

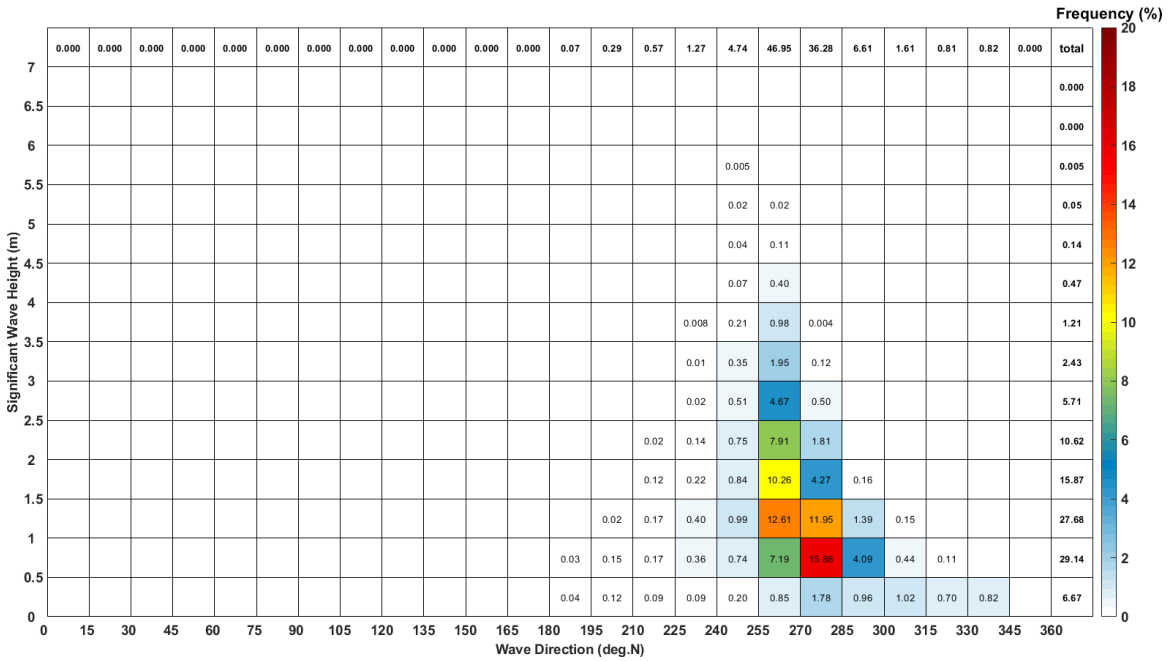

Hs \ Dir	0	15	30	45	60	75	90	105	120	135	150	165	180	195	210	225	240	255	270	285	300	315	330	345	360	total
7	0.000	0.000	0.000	0.000	0.000	0.000	0.000	0.000	0.000	0.000	0.000	0.000	0.000	0.07	0.29	0.57	1.27	4.74	46.95	36.28	6.61	1.61	0.81	0.82	0.000	total
6.5																										0.000
6																										0.000
5.5																		0.005								0.005
5																		0.02	0.02							0.05
4.5																		0.04	0.11							0.14
4																		0.07	0.40							0.47
3.5																	0.008	0.21	0.98	0.004						1.21
3																	0.01	0.35	1.95	0.12						2.43
2.5																	0.02	0.51	4.67	0.50						5.71
2																0.02	0.14	0.75	7.91	1.81						10.62
1.5																0.12	0.22	0.84	10.26	4.27	0.16					15.87
1														0.02	0.17	0.40	0.99	12.61	11.95	1.39	0.15					27.68
0.5													0.03	0.15	0.17	0.36	0.74	7.19	15.86	4.09	0.44	0.11				29.14
0													0.04	0.12	0.09	0.09	0.20	0.85	1.78	0.96	1.02	0.70	0.82			6.67

Table 3.6.2 *Annual-averaged wave data (2009-2019) at -20 m of location Center*

The results clearly indicate that the northgoing LST is strongly dominant for angles > 90° (north of Point Négade) The southgoing LST-values are only substantial for angles < 90° (south of Point Négade). The northgoing LST is maximum with a value of 1 to 1.5 million m^3/year around an angle of 125° (close to Barriquand). It should be realized that the LST-values represent sand transport capacity values. The actual LST are most likely smaller due to the presence of structures and limited availability of sand.

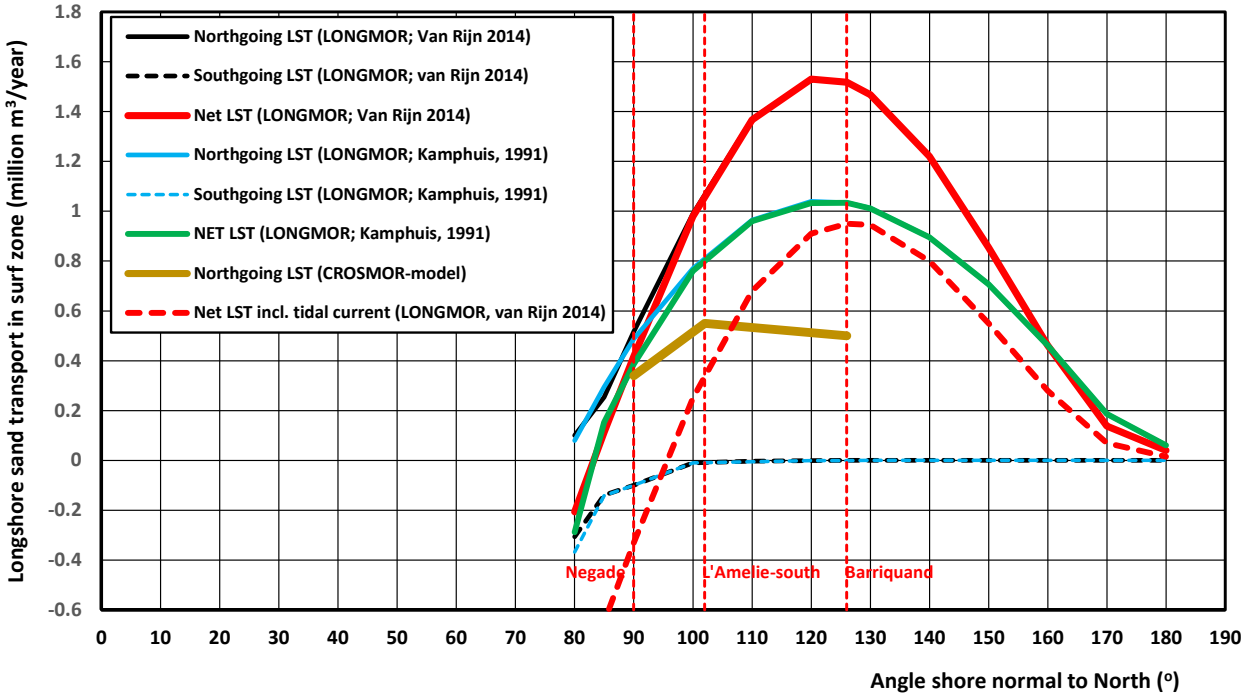

Figure 3.6.2 *Longshore sand transport at locations north of Point Négade, LONGMOR; d_{50}=0.35 mm*

Angle of shore normal (from sea to beach) to North (°)	Longshore sand transport (Mm^3/year) excluding tidal current Van Rijn (2014)			Longshore sand transport (Mm^3/year) Kamphuis (1991)			Longshore sand transport (Mm^3/year) Bayram et al. (2007)		
	North going	South going	Net	North going	South going	Net	North going	South going	Net
80	0.1	-0.306	-0.206	0.08	-0.368	-0.288	0.035	-0.85	-0.05
85	0.253	-0.14	0.133	0.294	-0.142	0.152	0.085	-0.035	0.05
90	0.517	-0.1	0.417	0.487	-0.1	0.387	0.173	-0.022	0.151
100	0.99	-0.01	0.98	0.77	-0.01	0.76	0.32	-0.017	0.31
110	1.37	-0.003	1.367	0.965	-0.005	0.96	0.41	-0.0005	0.41
120	1.531	-0.0006	1.5304	1.04	-0.001	1.033	0.42	-0.0001	0.42
126	1.519	-0.0002	1.5182	1.034	-0.0005	1.0335	0.4	0	0.4
130	1.468	-0.0001	1.4679	1.012	-0.0002	1.0118	0.37	0	0.37
140	1.22	0	1.22	0.895	-0.0001	0.8949	0.275	0	0.275
150	0.855	0	0.855	0.707	0	0.707	0.166	0	0.166
160	0.462	0	0.462	0.462	0	0.462	0.075	0	0.075
170	0.138	0	0.138	0.187	0	0.187	0.018	0	0.018
180	0.04	0	0.04	0.06	0	0.06	0.0045	0	0.0045

Angle shore normal to beach: Négade≅90°; L'Amélie-south≅103°; Barriquand≅126°
Transport coefficient Bayram=$(9+4H_{s,br}/(w_s T_p))10^{-5}$, w_s=0.06 m/s =settling velocity

Table 3.6.3 *Longshore sand transport (millions m^3/yr); north of Point Négade, LONGMOR; d_{50}=0.35 mm*

CROSMOR-model results

To get a better understanding of the wave and sand transport parameters along cross-shore bottom profiles, the CROSMOR-model has also been used (Files: SBAR1; SBAR2; SLAM1; SNEG1, Soulac1). This model has been applied to the cross-shore bottom profiles of Barriquand-northwest, L'Amélie-north, L'Amélie-south and Négade. The wave climate is based on location Center (**Table 3.6.2**) for Barriquand-northwest and location South for L'Amélie-north, L'Amélie-south and Négade. Six to seven wave cases including 90% of the wave energy are considered, see **Tables 3.6.4** to **3.6.7**.

The wave and transport parameter are computed for both HW (+1.7 m above mean sea level) and LW (-1.7 m). The effect of the tide level on LST is small. Model runs with and without tidal currents have been made. The tide-averaged and depth-averaged current velocity during the flood/ebb phases of the tide are represented by values of +0.3 m/s (flood to north) and -0.3 m/s (ebb to south). The results of the model runs with tidal currents have been used to derive the total sand transport on the shoreface (between -20 m and -5 m; seaward of the surf zone) as the total LST minus the LST in the surf zone.

The computed longshore sand transport values are, as follows (see also **Figure 3.6.4**):

Barriquand profile

- northgoing longshore sand transport in the surf zone (width up to 250 m) is about 0.5 M m^3/year (million m^3/year);
- total northgoing longshore sand transport increases to approximately 1.2 M m^3/year when the tidal current velocities are included;
- northgoing longshore sand transport in shoreface zone is about 0.7 M m^3/year;
- southgoing longshore sand transport in surf zone is absent;

L'Amelie-north

- northgoing longshore sand transport in the surf zone is about 0.55 M m^3/year (million m^3/year);
- total northgoing longshore sand transport increases to approximately 0.92 M m^3/year when the tidal current velocities are included;
- net northgoing longshore sand transport in shoreface zone is about 0.42 M m^3/year;
- southgoing longshore sand transport in surf zone is absent;

L'Amelie-south

- northgoing longshore sand transport in the surf zone is about 0.55 M m^3/year (million m^3/year);
- total northgoing longshore sand transport increases to approximately 0.7 M m^3/year when the tidal current velocities are included;
- net northgoing longshore sand transport in shoreface zone is about 0.25 M m^3/year; southgoing transport is increasing but smaller than northgoing transport);
- southgoing longshore sand transport in surf zone is absent;

Négade

- northgoing longshore sand transport in the surf zone is about 0.34 M m^3/year (million m^3/year);
- total northgoing longshore sand transport is about 0.32 M m^3/year when the tidal current velocities are included;
- northgoing and southgoing longshore sand transport in shoreface zone are almost equal (net transport is alnmost zero);
- southgoing longshore sand transport in surf zone is minor.

Figure 3.6.3 shows the cross-shore distribution of wave height, longshore current velocity and sand transport along the Barriquand-profile for Case WSW4 during HW and LW of **Table 3.6.4**. The longshore current velocity at the offshore boundary is set to 0.3 m/s (flood) to north during HW and -0.3 m/s to south (ebb) during LW.
Typical features are:

- nearshore wave height is somewhat smaller during LW due wave breaking effects;
- longshore current during LW is to south (negative values) on the shoreface and gradually decreases in landward direction due to bottom friction; maximum longshore current in the surf zone during LW is 0.35 m/s to north (current velocities change from south to north near the shore); maximum longshore current in the surf zone during HW is 0.55 m/s to the north;
- longshore sand transport on the shoreface is to the north during HW;
- longshore sand transport on the shoreface is also to the north during LW when the longshore current is to the south; this is caused by the wave asymmetry effect on the bed load transport generating a relatively strong north-going transport; the longshore transport on the shore face is to south when wave asymmetry effects are neglected;
- longshore sand transport in the surf zone with breaking waves is relatively high and always to the north as the waves come in from west-south-west

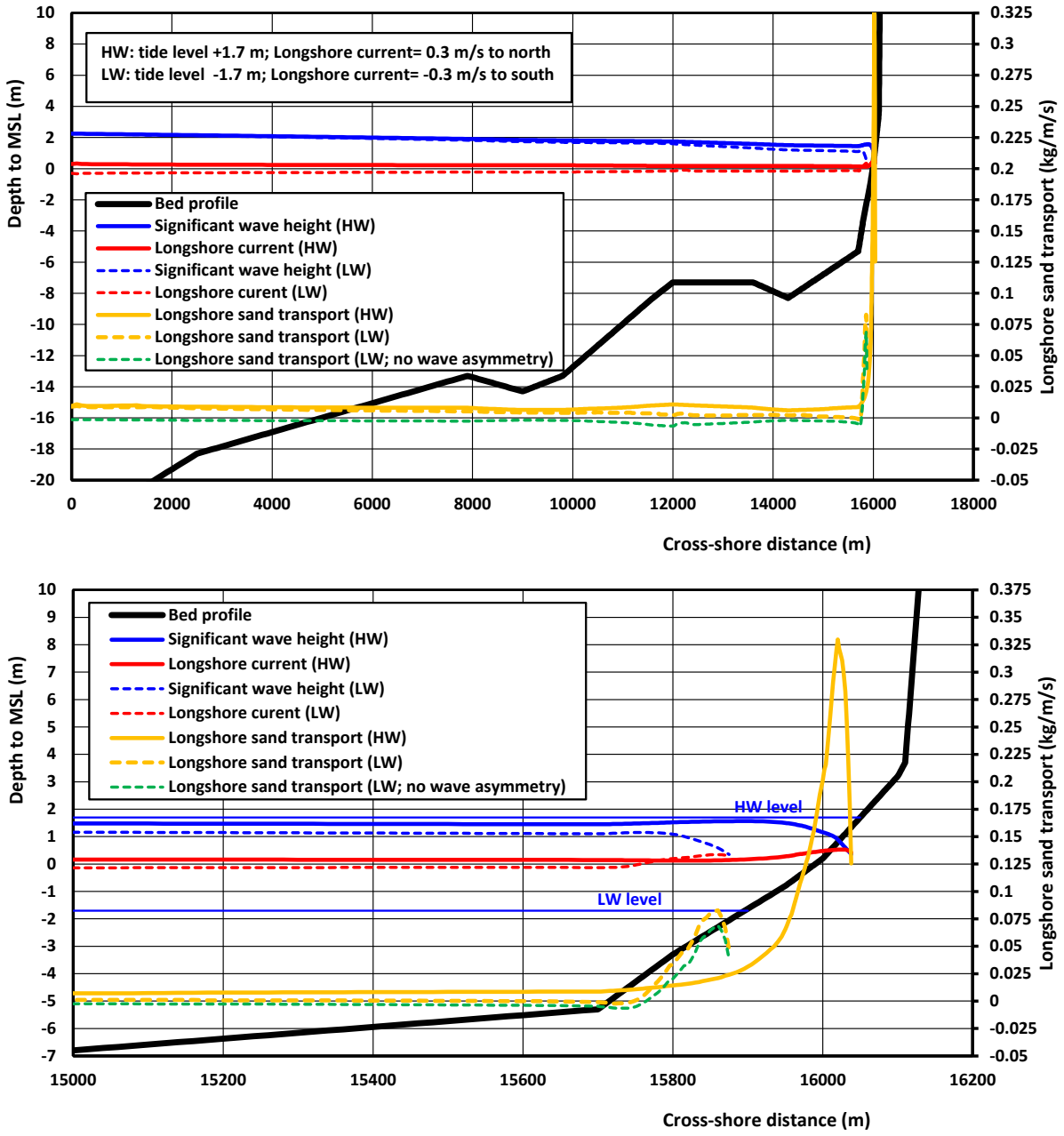

Figure 3.6.3 *Computed wave height, longshore current velocity and longshore sand transport along cross-shore profile Barriquand-northwest; Case WSW4; d_{50}=0.35 mm; CROSMOR-model*
Upper: deep water to shore profile; Lower: nearshore profile

Case	Offshore waves H_s (m) T_p (s) α (°)	Offshore wave incidence angle (°) to shore normal	Per cen tage occur rence p (%)	Tide level and longshore current velocity at offshore boundary	Waves at breaker line $H_{s,br}$ (m) α_{br} (°)	Maximum longshore and cross-shore current (m/s)	Surf zone width (m)	Longshore sand transport (m^3/year) +=northgoing -=southgoing	
								Exclu ding tidal current	Inclu ding tidal current
W1	0.75; 7; 275 (95)	31	27	HW +1.7 m; v=0.3 m/s	0.58; 9	0.15; -0.05	40	1,200	6,000
				LW -1.7 m; v=- 0.3 m/s	0.4; 8	0.05; -0.03	40	1,000	-5,000
W2	1.25; 9; 272 (92)	34	27	HW +1.7 m; v=0.3 m/s	0.9; 11	0.3; -0.1	70	10,000	33,000
				LW -1.7 m; v=-0.3 m/s	0.6; 9	0.15; -0.05	60	10,000	5,000
W3	1.75; 10; 268 (88)	38	15	HW +1.7 m; v=0.3 m/s	1.2; 14	0.4; -0.2	110	21,000	55,000
				LW -1.7 m; v=-0.3 m/s	0.8; 11.5	0.25; -0.1	100	21,,000	17,000
WSW4	2.25; 12; 265 (85)	41	10	HW +1.7 m; v=0.3 m/s	1.5; 17	0.55; -0.25	190	45000	150,000
				LW -1.7 m; v=-0.3 m/s	1.1; 15	0.35; -0.15	150	48,000	84,000
WSW1	3.0; 13; 262 (82)	44	8	HW +1.7 m; v=0.3 m/s	2.05; 20	0.7; -0.35	280	106,000	367,000
				LW -1.7 m; v=-0.3 m/s	1.6; 16	0.45; -0.2	160	110,000	195,000
WSW2	3.75; 14; 262 (82)	44	2	HW +1.7 m; v=-0.3 m/s	2.65; 21	0.9; -0.4	290	60,000	180,000
				LW -1.7 m; v=-0.3 m/s	1.8; 16	0.6; -0.25	170	63,000	83,000
Total								**0.5 Mm^3 to north**	**1.22 Mm^3 to north; 0.005 Mm3 to south**

α_o= offshore wave incidence angle to North; angle shore normal from beach to sea=306° (126°)
Tidal current positive = to north; Tidal current negative= to south

Table 3.6.4 *Computed longshore sand transport at Barriquand-northwest profile; d_{50}=0.35 mm; CROSMOR*

Case	Offshore waves H_s (m) T_p (s) α (°)	Offshore wave incidence angle (°) to shore normal	Percen tage occur rence p (%)	Tide level and longshore current velocity at offshore boundary	Longshore sand transport (m^3/year) +=northgoing -=southgoing	
					Excluding tidal current	Including tidal current
WNW1	0.75; 7; 275 (95)	31	31	HW +1.7 m; v=0.3 m/s	1,800	7,300
				LW -1.7 m; v=- 0.3 m/s	1,800	-4,500
WSW1	0.9; 9; 265 (85)	41	26	HW +1.7 m; v=0.3 m/s	11,000	36,000
				LW -1.7 m; v=-0.3 m/s	14,000	-500
WSW2	1.25; 10; 263 (83)	43	15	HW +1.7 m; v=0.3 m/s	25,000	68,000
				LW -1.7 m; v=-0.3 m/s	35,000	22,000
WSW3	1.6; 12; 260 (80)	46	10	HW +1.7 m; v=0.3 m/s	55,000	159,000
				LW -1.7 m; v=-0.3 m/s	79,000	82,000
WSW4	2.0; 13; 260 (80)	46	5	HW +1.7 m; v=0.3 m/s	67,000	172,000
				LW -1.7 m; v=-0.3 m/s	80,000	97,000
WSW5	2.35; 14; 260 (80)	46	2	HW +1.7 m; v=-0.3 m/s	52,000	113,000
				LW -1.7 m; v=-0.3 m/s	76,000	67,000
WSW6	3.05; 15; 255 (75)	51	0.5	HW +1.7 m; v=-0.3 m/s	33,000	55,000
				LW -1.7 m; v=-0.3 m/s	45,000	39,000
Total					**0.52 Mm^3 to north**	**0.92 Mm^3 to north; 0.005 Mm^3 to south**

α_o= offshore wave incidence angle to North; angle shore normal from beach to sea=306° (126°)

Table 3.6.5 *Computed longshore sand transport at L'Amelie north profile; d_{50}=0.35 mm; CROSMORl*

Case	Offshore waves H_s (m) T_p (s) α (°)	Offshore wave incidence angle (°) to shore normal	Percentage occurrence p (%)	Tide level and longshore current velocity at offshore boundary	Longshore sand transport (m^3/year) +=northgoing -=southgoing	
					Excluding tidal current	Including tidal current
WNW1	0.75; 7; 275 (95)	7	31	HW +1.7 m; v=0.3 m/s	1,200	6,000
				LW -1.7 m; v=- 0.3 m/s	1,500	-4,000
WSW1	0.9; 9; 265 (85)	17	26	HW +1.7 m; v=0.3 m/s	8,500	28,000
				LW -1.7 m; v=-0.3 m/s	15,000	-10,000
WSW2	1.25; 10; 263 (83)	19	15	HW +1.7 m; v=0.3 m/s	20,000	61,000
				LW -1.7 m; v=-0.3 m/s	30,000	6,600
WSW3	1.6; 12; 260 (80)	22	10	HW +1.7 m; v=0.3 m/s	50,000	140,000
				LW -1.7 m; v=-0.3 m/s	77,000	39,000
WSW4	2.0; 13; 260 (80)	22	5	HW +1.7 m; v=0.3 m/s	60,000	145,000
				LW -1.7 m; v=-0.3 m/s	93,000	53,000
WSW5	2.35; 14; 260 (80)	22	2	HW +1.7 m; v=-0.3 m/s	45,000	97,000
				LW -1.7 m; v=-0.3 m/s	65,000	40,000
WSW6	3.05; 15; 255 (75)	27	0.5	HW +1.7 m; v=-0.3 m/s	33,000	52,000
				LW -1.7 m; v=-0.3 m/s	45,000	32,000
Total					**0.55 Mm^3 to north**	**0.7 Mm^3 to north; 0.014 Mm^3 to south**

α_o= offshore wave incidence angle to North; angle shore normal from beach to sea=282° (102°)
Tidal current positive = to north; Tidal current negative= to south

Table 3.6.6 *Computed longshore sand transport at L'Amelie south profile; d_{50}=0.35 mm; CROSMOR*

Case	Offshore waves H_s (m) T_p (s) α (°)	Offshore wave incidence angle (°) to shore normal	Percentage occurrence p (%)	Tide level and longshore current velocity at offshore boundary	Longshore sand transport (m^3/year) +=northgoing -=southgoing	
					Excluding tidal current	Including tidal current
WNW1	0.75; 7; 275 (95)	-5	31	HW +1.7 m; v=0.3 m/s	-1,500	1,600
				LW -1.7 m; v=- 0.3 m/s	-600	-5,000
WSW1	0.9; 9; 265 (85)	5	26	HW +1.7 m; v=0.3 m/s	8,500	20,000
				LW -1.7 m; v=-0.3 m/s	4,900	-14,000
WSW2	1.25; 10; 263 (83)	7	15	HW +1.7 m; v=0.3 m/s	17,000	39,000
				LW -1.7 m; v=-0.3 m/s	12,000	-20,000
WSW3	1.6; 12; 260 (80)	10	10	HW +1.7 m; v=0.3 m/s	36,000	83,000
				LW -1.7 m; v=-0.3 m/s	29,000	-8,000
WSW4	2.0; 13; 260 (80)	10	5	HW +1.7 m; v=0.3 m/s	39,000	86,000
				LW -1.7 m; v=-0.3 m/s	34,000	1,000
WSW5	2.35; 14; 260 (80)	10	2	HW +1.7 m; v=-0.3 m/s	23,000	48,000
				LW -1.7 m; v=-0.3 m/s	21,000	2,000
WSW6	3.05; 15; 255 (75)	15	0.5	HW +1.7 m; v=-0.3 m/s	18,000	30,000
				LW -1.7 m; v=-0.3 m/s	19,000	10,000
Total					**0.34 Mm^3 to north**	**0.32 Mm^3 to north; 0.047 Mm^3 to south**

α_o= offshore wave incidence angle to North; angle shore normal from beach to sea =270° (90°)

Table 3.6.7 *Computed longshore sand transport at Négade profile; d_{50}=0.35 mm;Crosmorl*

Best estimate of longshore sand transport

Information of the north-going longshore sand transport (LST) from earlier studies shows values between 0.1 and 0.6 Mm^3/year.

The results of the LONGMOR and CROSMOR-models indicate values in the range of 0.3 to 1.5 Mm^3/year in the surf and shoreface zone between Négade and Barriquand. The LST values of the CROSMOR-model are more realistic than the values of the LONGMOR-model, as the actual cross-shore bottom profile is taken into account. The CROSMOR-model also produces LST-values in the shoreface zone.
Based on this, the best estimate of the LST in the surf and shoreface zones are shown in **Figure 3.6.4** and in **Table 3.2.8**. The north-going LST in the surf zone increases from south to north due to an increasing wave incidence angle with respect to the coastline angle. South of Négade is a point of zero LST (divergence point or null point). The maximum LST of about 0.6 Mm^3/year is in good agreement with the annual erosion volume of about 0.7 Mm^3/year between Négade and Le Signal.
It should be realized that the values given in Figure 3.6.4 for the surf zone are sand transport capacity values in conditions with unlimited supply of sand (long and straight beaches; wide and high beaches; multiple breaker bars).
The coastal section of Soulac and adjacent beaches has a northern boundary at the inlet and a southern boundary at Négade, where the longshore sand transport is almost zero (null point). The total length of this coastal section is about 11 km. Most of the sand supply comes from dune erosion in two regions: Négade-L'Amelie (1.5 km) and L'Amélie-Camping LS (1.5 km). The actual net longshore sand transport at Soulac beach is unknown, but is less than the longshore sand transport capacity and is estimated to be about 300,000 $\pm$ 150,000 m^3/year.
In the future, the longshore sand transport at Soulac beach may be substantially smaller if measures (dune revetments) are taken to reduce the dune erosion between Négade and Camping Les Sables.

Figure 3.6.4 *Net annual longshore sand transport values in shoreface zone (seaward of -5 m depth) and in surf zone (landward of -5m depth line)*

Coastal sand transport	Coastal section L'Amelie to Soulac sur Mer		
	Between LAT and HAT (active layer≅ 5 m)	**Between LAT and -5 m CDL**	**Between -5 m and -25 m CD**
Net annual longshore sand transport (NALT) excluding tidal currents (m^3/year)	lower limit-upper limit 100.000-200.000	100.000-200.000	<100.000
Net annual longshore sand transport (NALT) including tidal currents (m^3/year)	150.000-300.000	150.000-300.000	300.000-600.000

Table 3.6.8 *Best estimates of longshore sand transport in coastal zone between L'Amelie and Soulac sur Mer (sand 0.35 mm); (MSL= mean sea level; LAT≅2.5 m below MSL; HAT≅2.5 m above MSL)*

3.6.2 Coastline hindcast 2014-2021

The LONGMOR-model has been used to hindcast the coastline changes between 2014 and 2021 (5 years), which is the period after extension (with 80 m) of the Barriquand-groin in 2014 (**Figure 3.6.5**). The coastline is defined as the MSL-line (MSL=Mean Sea Level). The model domain extends over about 6 km south of the Barriquand-groin. The tip of the Barriquand-groin is landward of LAT-line (about 2.5 m below MSL).
The model input data are given in **Table 3.6.9**. The angle between the main wave direction and the shore normal varies between 15° (L'Amélie) and 30° (Barriquand).

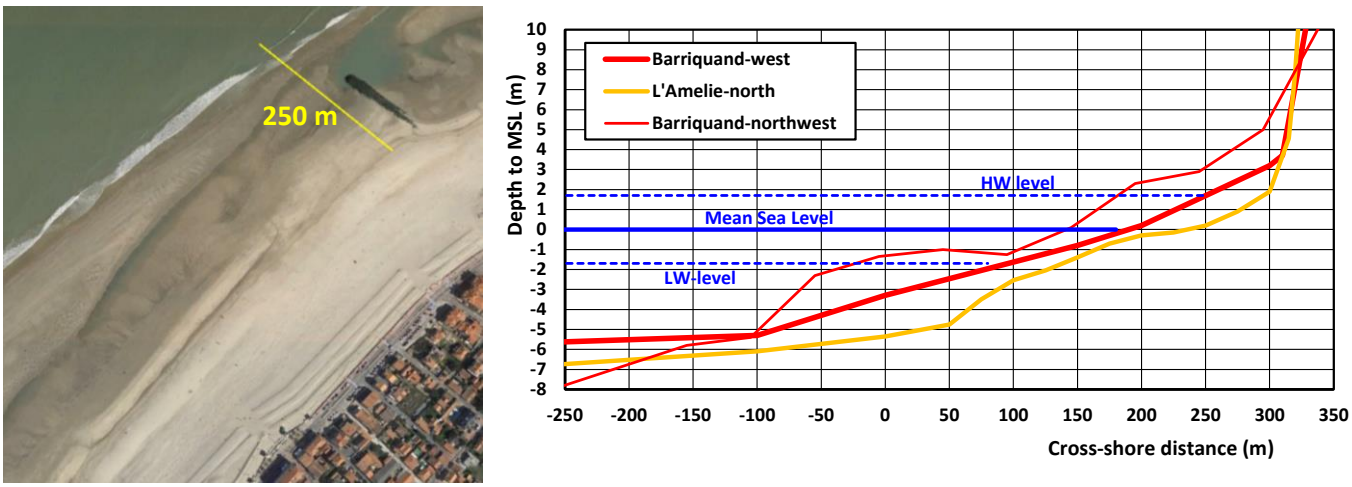

Figure 3.6.5 *Width of surf zone near Barriquand-groin seaward of MSL line*

Preliminary model runs

Preliminary model runs have been performed based the simplified coastline (2014) derived from Google Earth imagery. The two most important parameters are the net annual langshore sand transport (NALT) and the percentage of bypassing sand transport (BPP) over and along the tip of the groin. The NALT is asumed to be in the range of 150,000 m^3/year landward of LAT-line (active layer=5 m) to 500.000 m^3/year landward of -5 m depth line below MSL (active layer of 10 m), based on a (separate) detailed study of longshore sand transport for representative wave conditions and tidal currents. The BPP is estimated to be in the range of 40% to 75%, as the existing groin is situated landward of the LAT depth contour, whereas the surf zone extends to the -5 m depth contour. Furthermore, sand will be carried over the groin during storm conditions.

Preliminary model runs have been made for four cases:

- Case A: NALT=300,000 m^3/year and BPP=60%; offshore wave incidence angle=30°; Layer= 10 m;
- Case B: NALT=300,000 m^3/year and BPP=60%; offshore wave incidence angle=15°; Layer= 10 m;
- Case C: NALT=500,000 m^3/year and BPP=75%; offshore wave incidence angle=30°; Layer= 10 m;
- Case D: NALT=150,000 m^3/year and BPP=60%; offshore wave incidence angle=30°; Layer= 5 m.

The results of Case A to D are shown in **Figure 3.6.6**.
Case A to D yield similar results. The maximum accretion over 5 years close to the groin is about 60 m, which is slightly less than the extension (80 m) of 2014. The total sand deposition volume of Case D is about 210.000 m^3 over 5 years
Summarizing, it is noted that similar results can be obtained by different settings of the (many) free input parameters inherent of a relatively simple 1D-model approach. Based on these results, the net longshore sand transport at Soulac is estimated to be of the order of 200,000 $\pm$ 50,000 m^3/year landward of the LAT-line.

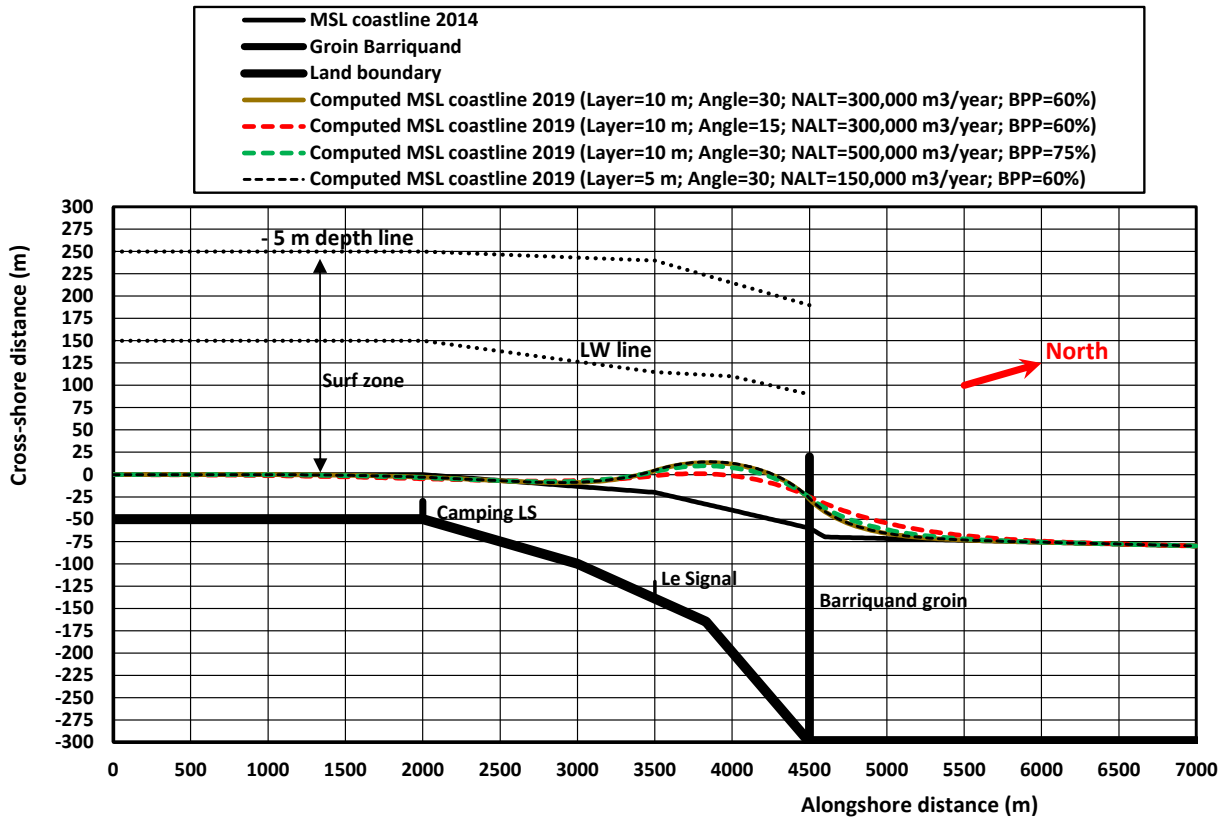

Figure 3.6.6 *Computed coastline changes in region Soulac sur Mer 2014-2019; LONGMOR-model*

PARAMETER	VALUES
Offshore significant wave height	1.5 m (100% of the time)
Offshore wave angle of main wave direction	15°; 30°
Peak wave period	8 s
Grid size and domain length	20 m; 4500 m
Time step and grid-'smoothing'	0.01 day
Sand d_{50}, d_{90}	0.35; 1 mm
Slope beach-surf zone 0 tot -5 m MSL	1 to 50 (tan slope=0.02)
Breaker coefficient	0.7
Layer thickness of active zone	10 m (between -5 m and +5 m to MSL) 5 m (between LAT and HAT)
Longshore transport equation; Calibration coefficient K	Van Rijn 2014; K=variable
Net annual longshore transport (NALT) landward of LAT and bypassing percentage	NALT=200,00-300,000 m^3/year; BPP=40%-60%
Net annual longshore transport (NALT) landward of -5 m depth and bypassing percentage	NALT=400,000 -600,000 m^3/year; BPP=60%-75%
Angle of coast normal to North (from beach to sea)	285 to 305 degrees
Tidal currents in surf zone	V_{flood}=0 m/s; V_{ebb}=0 m/s (no effect if both values are equal)
Beach nourishment volume	based on Table 3.3.2
Input files	Soul1.inp (preliminary runs) Soul1d.inp (detailed calibration runs)

Table 3.6.9 *Input data of LONGMOR-model; Soulac sur Mer.*

Detailed calibration runs

The detailed coastlines (MSL, HAT, LAT, 5 m depth) of 2014, 2017 and 2020 supplied by the client are shown in **Figure 3.6.7**. The origin (x=0) is the groin north of L'Amélie. The model was calibrated by varying the K-coefficient of the longshore sand transport in the active layer of 5 m (between LAT and HAT). Detailed model runs have been made with and without local sand replacements (excavation and dumping of beach sand. The sand replacements were done by 7 trucks carrying 15 m^3 of sand each working 6 hours a day (3 hours before and after low tide). Sand was extracted close to the Barriquand-groin and dumped near Camping LS. Production was 10,000 m^3 per week and maximum 60,000 m^3 over a period of 6 weeks in spring (March, April, May). In total, about 200,000 m^3 of sand has been replaced between 2018 and 2021.

Figure 3.6.7 also shows hindcasted MSL-coastlines between 2014 and 2021 excluding and including local sand replacements based on the values from **Table 3.6.10**. Very reasonable agreement can be observed between the predicted MSL-coastline of September 2021 (including sand replacements) and measured MSL-coastline of May 2020.

Major erosion (about 300,000 m^3 over 7 years with sand replacements) occurs in the section between L'Amélie and Camping LS, which is caused by the change of the coastline north of L'Amélie with respect to the coastline south of L'Amélie resulting in a significant increase of NALT.

Deposition of sand (about 600,000 m^3 over 7 years without sand replacements) prevails between Le Signal and Barriquand-groin (x=2200 to x=3700 m). The deposition north of the Barriquand-groin is about 125,000 m^3 over 7 years due to bypassing processes. The computed erosion volume in the section north of L'Amélie between x=0 and x=2200 m is about 300,000 m^3 over 7 years. The net deposition volume between x=0 and x=6000 m is about 600,000+125,000-300,000=425,000 m^3 over 7 years or about 60,000 m^3/year which is about equal to the difference (170,000-110,000 m^3/year) in longshore sand transport between x=0 and x=6000 m (**Figure 3.6.8**).

The maximum predicted accretion including sand replacement is about 100 m at x=3500 m. The MSL line is far seaward of the tip of the groin at that location (x=3500 m). The replacement of sand from section 3300-3800 m to section 1150-2300 m in the period 2018 to 2021 mitigates the erosion around Camping LS.

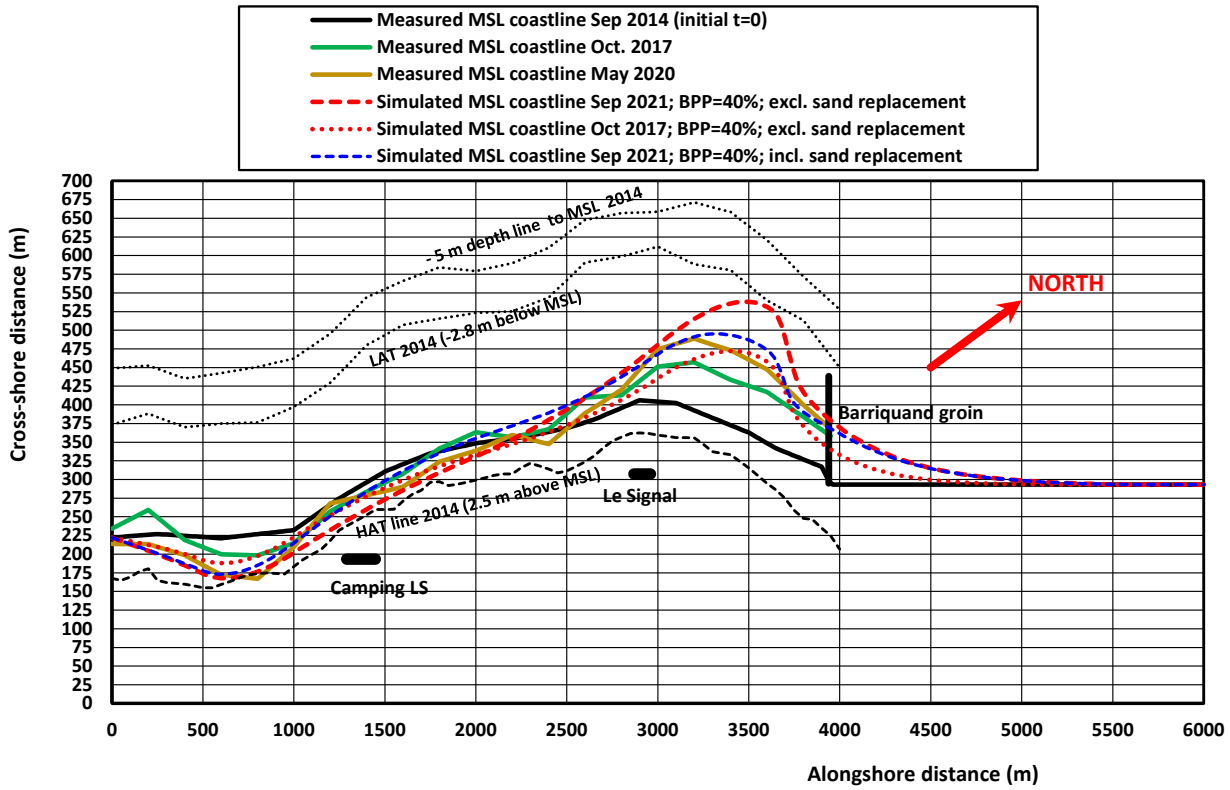

Figure 3.6.7 *Computed coastline changes in region Soulac sur Mer 2014-2020; detailed calibration of LONGMOR-model*

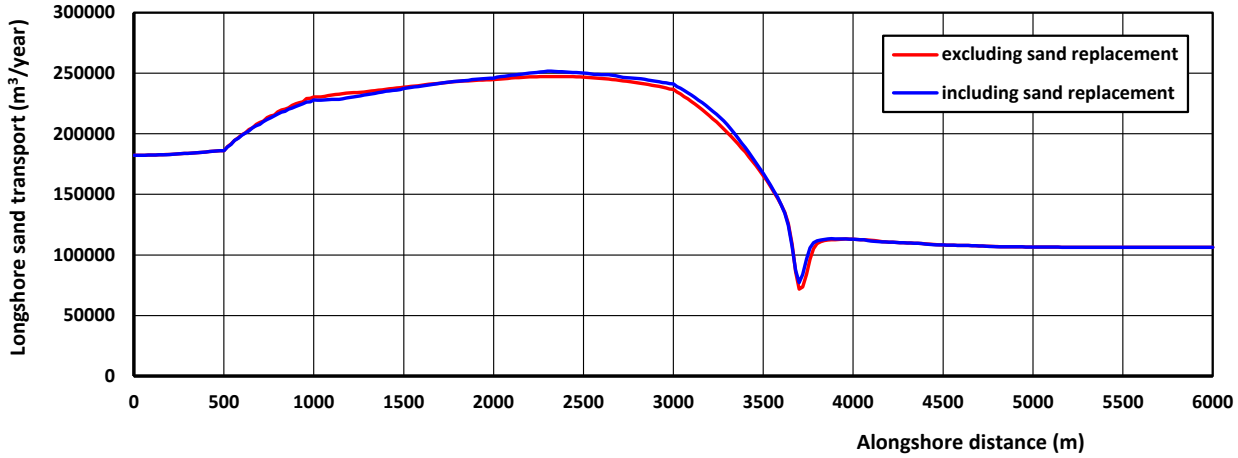

Figure 3.6.8 *Computed longshore sand transport landward of the LAT-line; detailed calibration of LONGMOR-model*

Figure 3.6.8 shows the net longshore sand transport (NALT) landward of the LAT-line and averaged over the period September 2014 to September 2021.

The NALT at the origin is about 170,000 m^3/year which increases to 250,000 m^3/year around Le Signal and decreases to 110,000 m^3/year between Le Signal and Barriquand-groin (x=2500 to 4000 m). The bypassing longshore transport is about 110,000 m^3/year, which is about 45% of the updrift value of 250,000 m^3/year. The increase of NALT between x=0 and x=2200 m is caused by the change of the coastline north of L'Amélie with respect to the coastline south of L'Amélie. The overall NALT-value over the length of the domain decreases by about 60,000 m^3/year or a total net deposition volume about 420,000 m^3 over 7 years.

Date	Volume (m^3)	Volume per unit length and time (m^3/m/day)	Excavation location	Dumping location
October-November 2018 (60 days)	40,000	-1.33/0.83	x=3300-3800 m	x=1500-2300
	5,000	-0.17/0.55	x=3300-3800 m	x=2850-3000
April-May 2019 (60 days)	40,000	-1.33/0.83	x=3300-3800 m	x=1500-2300
May-June 2020 (60 days)	60,000	-2/0.87	x=3300-3800 m	x=1150-2300
April-May 2021 (60 days)	60,000	-2/0.87	x=3300-3800 m	x=1150-2300

Table 3.6.10 *Excavation and dumping volumes of beach sand (- =extraction; +=dumping)*

3.6.3 Design of groyne extension at Barriquand

Varions runs have been made for a longer groyne at Barriquand, see **Figure 3.6.9**.
Figure 3.6.10 shows the net longshore sand transport (NALT) landward of the LAT-line and averaged over the computation period.

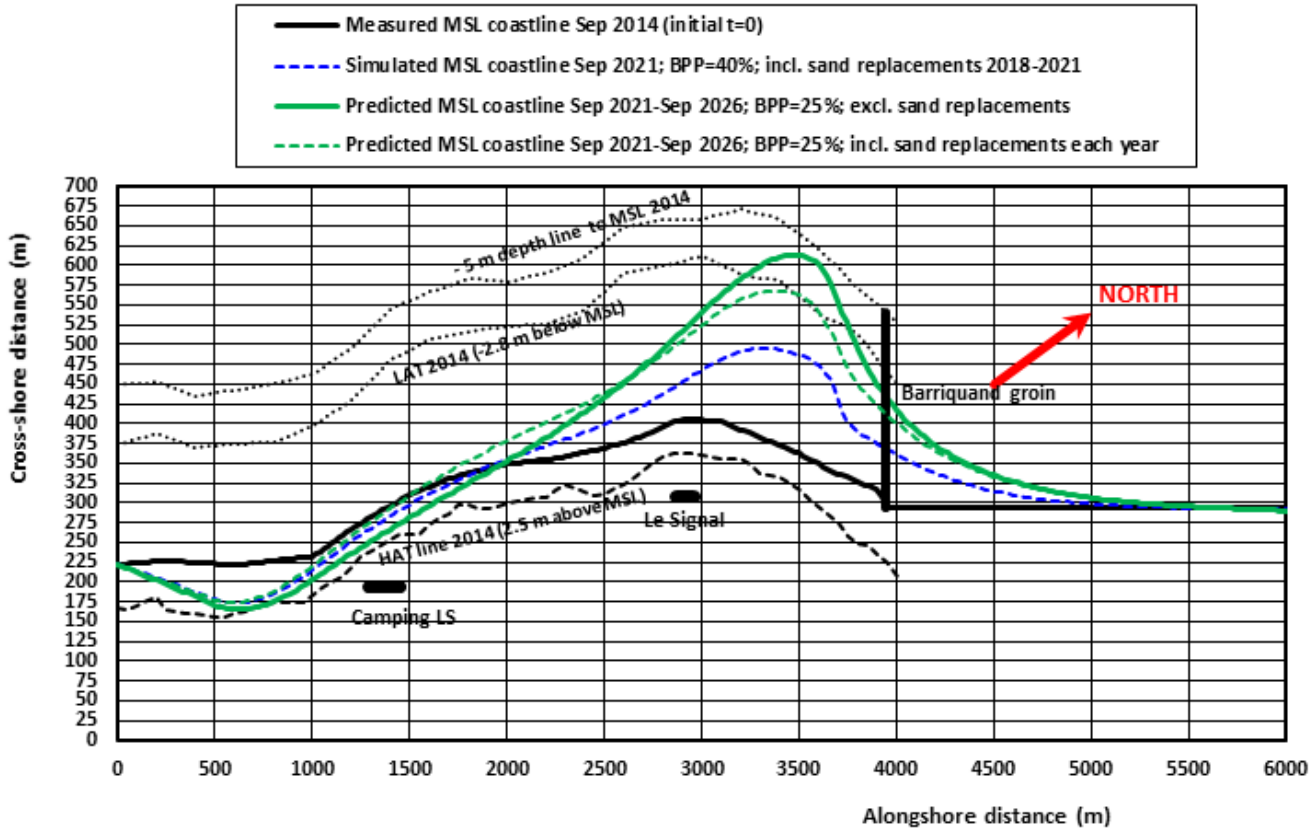

Figure 3.6.9 *Computed coastline changes in region Soulac sur Mer 2014-2020; longer groyne*

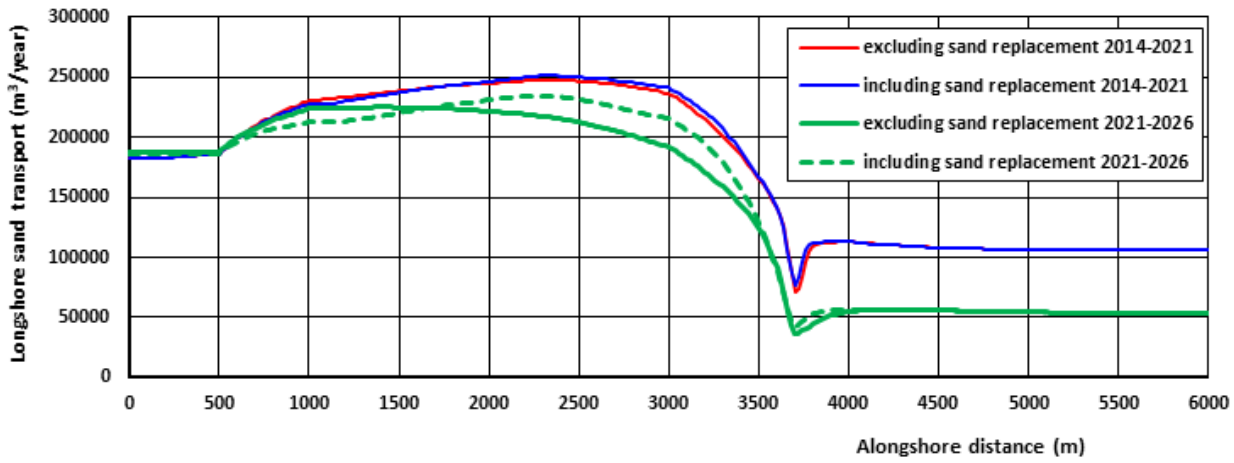

Figure 3.6.10 *Computed longshore sand transport landward of the LAT-line; longer groyne*

3.6.4 New groin at Boulevard Des Dunes

Analternative option (C) is a new groin at boulevard Des Dunes at about 2500 m from the origin
The detailed coastlines (MSL, HAT, LAT, 5 m depth) of 2014, 2017 and 2020 supplied by the client are shown in **Figure 3.6.11**. The origin (x=0) is the groin north of L'Amélie. The model was calibrated by varying the K-coefficient of the longshore sand transport in the active layer of 5 m (between LAT and HAT).
The LONGMOR-model of LVRS Consultancy has been used to predict the coastline development between Camping LS and Barriquand-groin at Soulac-beach over a period of 10 to 15 years (2020-2035) without beach nourishment or sand replacements.
Three cases are considered, as follows:

- initial coastline May 2020; predicted coastline 2030
  bypassing percentage Des Dunes-groin=85%;
  bypassing percentage Barriquand groin=75%;
- initial coastline May 2020; predicted coastline 2030
  bypassing percentage Des Dunes-groin=85%;
  bypassing percentage Barriquand groin=90%;
- initial coastline May 2020; predicted coastline 2035
  bypassing percentage Des Dunes-groin=70%;
  bypassing percentage Barriquand groin=90%.

The input data and settings (based on calibration runs) are given in **Table 3.6.11**. The bypassing values are based on detailed computations of the Telemac-model system including the new groin and the Barriquand-groin.

PARAMETER	VALUES
Offshore significant wave height	1.5 m (100% of the time)
Offshore wave angle of main wave direction	15°; 30°
Peak wave period	8 s
Grid size and domain length	20 m; 4500 m
Time step and grid-'smoothing'	0.02 day; 0.005
Sand d_{50}, d_{90}	0.35; 1 mm
Slope beach-surf zone 0 tot -5 m MSL	1 to 50 (tan slope=0.02)
Breaker coefficient	0.7
Layer thickness of active zone	5 m (between LAT and HAT)
Longshore transport equation; Calibration coefficient K	Van Rijn 2014; K=variable
Net annual longshore transport (NALT) landward of LAT and bypassing percentage	NALT=200,00-300,000 m^3/year; BPP at new DD-groin=70%-85%
Angle of coast normal to North (from beach to sea)	285 to 305 degrees
Tidal currents in surf zone	V_{flood}=0 m/s; V_{ebb}=0 m/s (no effect if both values are equal)
Beach nourishment volume	none
Input files	SoulDD1.inp

Table 3.6.11 *Input data of LONGMOR-model; Soulac sur Mer.*

Figure 3.6.11 shows predicted coastline for the three case of Option C.

Figure 3.6.12 shows the net longshore sand transport along the domain of 6 km. The total volume of sand trapped over the domain of 6000 m is 185,000-145,000= 40,000 m^3 per year, or about 400,000 m^3 over 10 years. This low trapping value is caused by the relatively high bypassing percentages
The results are, as follows:

- coastal accretion of about 300,000 m^3 over 10 years southward of the new groin at Boulevard DD;
- erosion of sand of about 150,000 m^3 over 10 years in the middle part between the new groin and the Barriquand-groin; accretion of about 150,000 m^3 over 10 years at both ends of the compartment between the two groins; sand volume between groins is redistributed;
- coastal accretion of about 75,000 m^3 over 10 years northward of the Barriquand-groin.

The accretion at south updrift side of new groin does not increase much in the period 2030 to 2035, because the coastline at the updrift side of the new groin becomes gradually normal to the incoming waves.

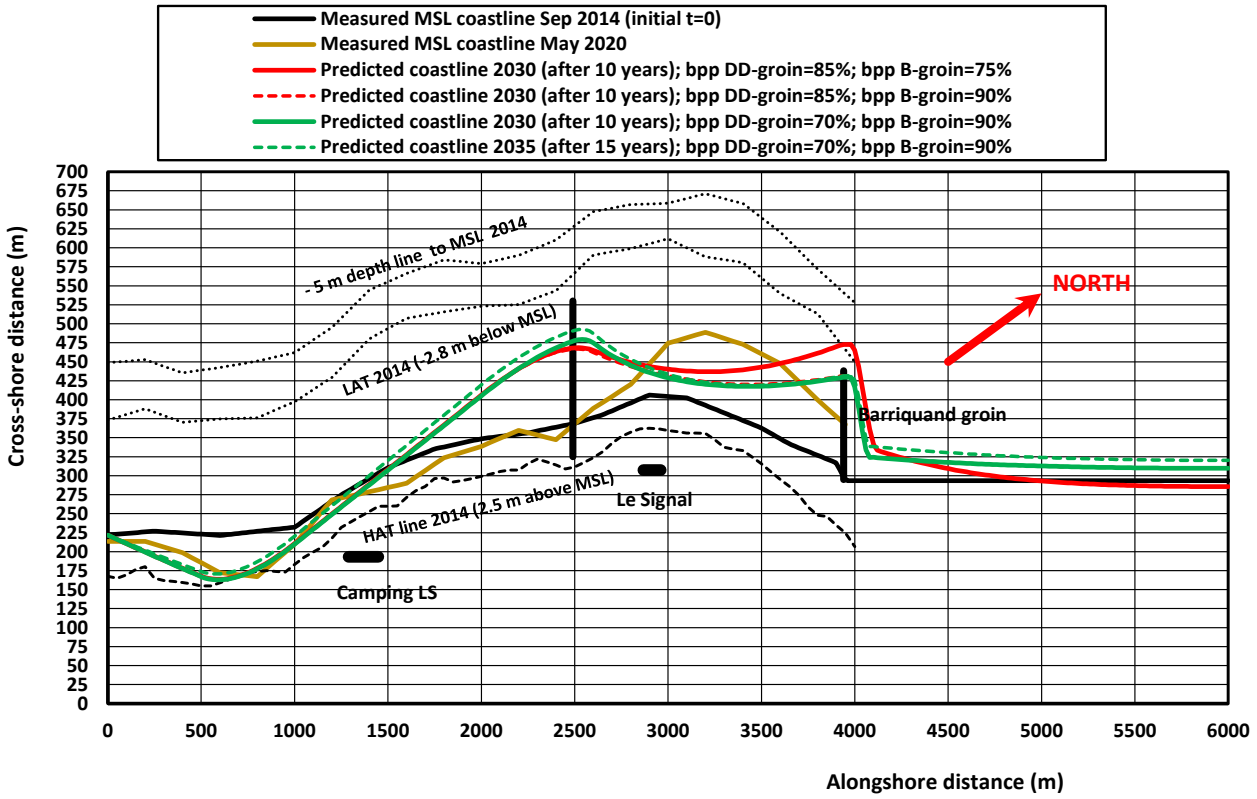

Figure 3.6.11 *Predicted coastline development in period 2020-2035; Option C; Net longshore sand transport at origin = 185,000 m³/year; LONGMOR-model (soulDD1.inp)*

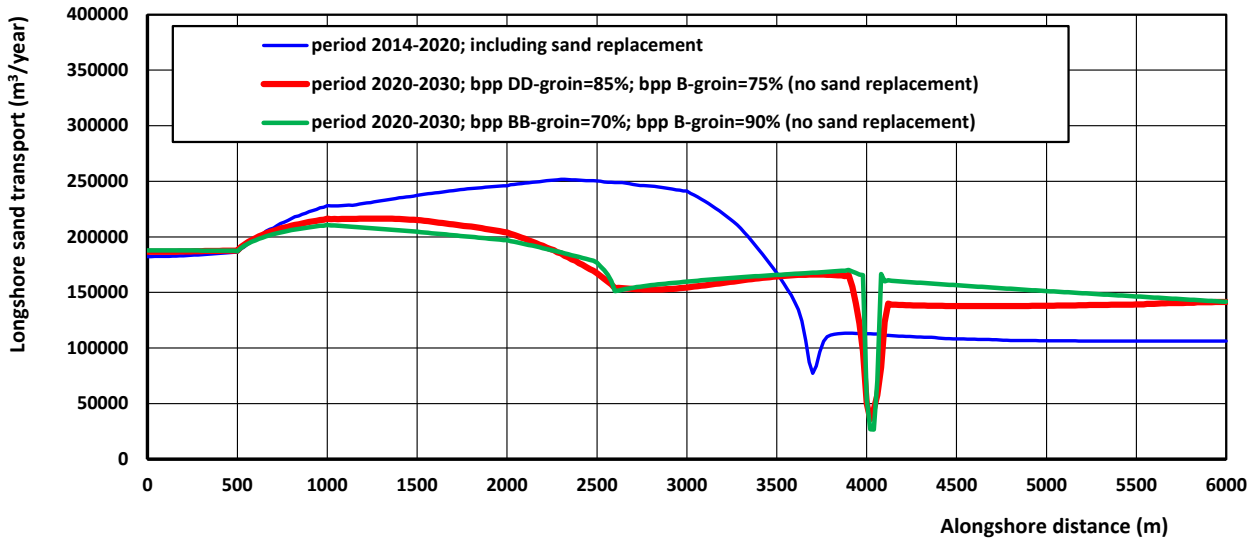

Figure 3.6.12 *Computed annual-averaged longshore sand transport landward of the LAT-line; new dune*

4. References

Kamphuis, J.W. 1991. Alongshore sediment transport rate. Journal of Waterway, Port, Coastal and Ocean Engineering, Vol. 117, p. 624-640

Kamphuis, J.W. 1992. Short course on design and reliability of coastal structures. Chapter 9, Proc. 23rd ICCE, Venice, Italy.

Shore Protection Manual, 1984. CERC, Waterways Experiment Station, Vicksburg, USA

Van Rijn, L.C., 1990, 2011. Principles of fluid flow and surface waves in rivers, estuaries and coastal seas. www.leovanrijn-sediment.com.

Van Rijn, L.C., 1993. Principles of sediment transport in rivers, estuaries and coastal seas. www.leovanrijn-sediment.com.

Van Rijn, L.C., 1998. Principles of coastal morphology. www.leovanrijn-sediment.com.

Van Rijn, L.C., 2002. Longshore sand transport. Proc. 28th ICCE, Cardiff, U.K.

Van Rijn, L.C., 2005, 2017. Principles of sedimentation and erosion engineering in rivers, estuaries and coastal seas. www.leovanrijn-sediment.com

Van Rijn, L.C., 2014. A simple general expression for longshore transport of sand, gravel and shingle. Coastal Engineering, 90, 23-39

Van Rijn, L.C., 2015. Coastal erosion in lee zone of structure. www.leovanrijn-sediment.com